



UNIVERSITY OF <sup>TM</sup>  
KWAZULU-NATAL

---

INYUVESI  
YAKWAZULU-NATALI

**ENERGY HARVESTING BY VIBRATION USING  
PIEZOCERAMIC MATERIALS (PZT-4)**

Submitted by

**Lumbumba Taty-Etienne Nyamayoka**  
**(Student Number: 212562545)**

Supervisor: Dr Freddie L. Inambao

**November 2014**

---



UNIVERSITY OF <sup>TM</sup>  
**KWAZULU-NATAL**

---

INYUVESI  
**YAKWAZULU-NATALI**

**ENERGY HARVESTING BY VIBRATION USING  
PIEZOCERAMIC MATERIALS (PZT-4)**

Submitted by

**Lumbumba Taty-Etienne Nyamayoka**  
**(Student Number: 212562545)**

Submitted in fulfilment of the academic requirements for the degree of Master  
of Science in Mechanical Engineering

**Supervisor: Dr Freddie L. Inambao**

School of Engineering, University of KwaZulu-Natal, Durban, South Africa

November 2014

---

“As the candidate’s supervisor, I agree/~~do not agree~~ to the submission of this thesis. The supervisor must sign all copies after deleting which is not applicable.”

.....**DR Freddie L. Inambao**.....

NAME OF SUPERVISOR

...  ...

SIGNATURE

# DECLARATION 1                      PLAGIARISM

I, **Lumbumba Taty-Etienne Nyamayoka** declare that

1. The research reported in this thesis, except where otherwise indicated, is my original research.
2. This thesis has not been submitted for any degree or examination at any other university.
3. This thesis does not contain other persons' data, pictures, graphs or other information, unless specifically acknowledged as being sourced from other persons.
4. This thesis does not contain other persons' writing, unless specifically acknowledged as being sourced from other researchers. Where other written sources have been quoted, then:
  - a. Their words have been re-written but the general information attributed to them has been referenced;
  - b. Where their exact words have been used, then their writing has been placed in italics and inside quotation marks, and referenced.
5. This thesis does not contain text, graphics or tables copied and pasted from the Internet, unless specifically acknowledged, and the source being detailed in the thesis and in the References sections.

Signed

...  ...

## DECLARATION 2                      PUBLICATIONS

DETAILS OF CONTRIBUTION TO PUBLICATIONS that form part and/or include research presented in this thesis (include publications in preparation, submitted, in press and published and give details of the contributions of each author to the experimental work and writing of each publication)

Publication 1: **L. T-E. Nyamayoka** and **F. L. Inambao**: “Performance characteristic of piezoelectric energy harvesting devise,” Presented at 13<sup>th</sup> International Conference on Sustainable Energy Technologies 25<sup>th</sup> - 28<sup>th</sup> August 2014 HES-SO – Geneva - Switzerland ([www.hes-so.ch/set2014](http://www.hes-so.ch/set2014)), 2014.

Publication 2: **L. T-E. Nyamayoka** and **F. L. Inambao**: “A review of vibration energy harvesting, technique and application,” in *Proceedings of 13<sup>th</sup> Botswana Institution of Engineering Biennial Conference 978-99912-0-910-4*, 15<sup>th</sup> - 18<sup>th</sup> October 2013, Gaborone, Botswana, pp. 14-22.

Publication 3: **L. T-E. Nyamayoka**, **G.A. Adewumi** and **F. L. Inambao** “Fabrication and performance of MEMS-based piezoelectric power generation for vibration energy harvesting” *International Journal of Low-Carbon Technologies* (submitted for publication).

**In all these papers, I Lumbumba T-E. Nyamayoka was the main and corresponding author, whilst Dr Freddie L. Inambao was the co-author and my research supervisor.**

Signed

...  ...

## ACKNOWLEDGEMENTS

I would like to thank God, the Lord almighty for giving me the strength to start, and without whom none of this would have been possible.

A number of people were responsible for the success of this project and the presentation of this thesis. I would like to express my special appreciation and thanks to my advisor and supervisor **Dr. Freddie L. Inambao**, you have been a tremendous mentor for me. I would like to thank you for encouraging my research and for allowing me to grow as a research scientist. Your advice on both research as well as on my career have been priceless. I would also like to thank the Discipline of Mechanical Engineering Staff for their assistance and advice even at hard times. I would especially like to thank the staff at the Vibration Research Testing Centre (Westville campus, University of KwaZulu-Natal) for providing the availability of the laboratory and for assisting with technical information. All of you supporting me when I collected experimental data for my thesis.

I would also like to acknowledge the financial assistance of the Centre for Engineering Postgraduate Studies for funding me during my stay at UKZN, in particular **Professor Nelson M. Ijumba**. I would also like to express my heartfelt thanks to all my colleagues in the Green Energy Solution Research Group for making helpful suggestions throughout the duration of my study and also my housemates **Grace Kayumba** and **Alain Kabwit** for their support and friendship.

A special thanks to my family. Words cannot express how grateful I am to my father and mother for all of the sacrifices that you've made on my behalf. Your prayers for me were what sustained me thus far.

Finally I would like to thank all those who have contributed, and supported me in writing, and inspired me either directly or indirectly to strive towards my goals.

## **ABSTRACT**

The concept of energy harvesting in the ambient environment is of great interest. Energy harvesting is the process of drawing out a small amount of energy from the ambient environment. The ambient environment is characterized by various available sources of energy such as solar, wind, vibration, gas, liquid flows, etc., which can be converted to usable energy. Vibration energy harvesting is a mechanical process of gathering ambient energy from vibrating sources that can be converted into electrical energy using different techniques of conversion. Vibration energy is available in the urban and industrial environment, but it is often overlooked as a source of power to be scavenged and to provide electricity. There are various techniques for conversion of harvesting ambient energy found in nature. The main harvesting techniques are electromagnetic conversion, electrostatic conversion and piezoelectric conversion.

In this context, this research study is concerned with finding a way to harvest electrical energy from vibration. Piezoelectric conversion is able to produce high electrical energy unlike electromagnetic and electrostatic conversion. Piezoelectric materials have a large capacity for conversion of energy due to their inherent ability to detect vibration sources. This conversion of mechanical energy to electrical energy through the use of piezoelectric materials is an exciting and rapidly developing area of research with a widening range of applications constantly materializing.

The experiments for this study were performed at the Vibration Research and Testing Centre (VRTC) laboratory of the University of KwaZulu-Natal, Durban. An electrodynamic vibration (shaker) connected to the prototype (cantilever beam plus piezoelectric material, i.e. ceramic plate PZT-4) was used to simulate ambient vibration to collect the data. The experiments were designed to optimise power output of the prototype by estimating the output voltage. Two setups of prototype were used: a cantilever beam with a tip mass at the end and a cantilever beam without tip mass at the end. Data from the experiment was compared and analysed using MatLab. The results showed that the power output of the prototype with the tip mass was greater than the power output without the tip mass. The

results of this study contribute to the development of piezoelectric power generation as a viable source of electrical energy with minimal environment impact.

*Keywords: Energy harvesting, Energy conversion, Piezoelectricity, Piezoelectric material, Electromagnetic conversion, Electrostatic conversion, Piezoelectric conversion.*



# TABLE OF CONTENTS

DECLARATION 1 PLAGIARISM .....	ii
DECLARATION 2 PUBLICATIONS.....	iii
ACKNOWLEDGEMENTS.....	iv
ABSTRACT.....	v
TABLE OF CONTENTS.....	vii
LIST OF FIGURES .....	x
LIST OF TABLES.....	xii
NOMENCLATURE .....	xiii
ACRONYMS AND ABBREVIATIONS .....	xvii
CHAPTER ONE INTRODUCTION.....	1
1.1 Background .....	1
1.2 Motivation for this research .....	2
1.3 Research questions .....	3
1.4 Aim and objectives of this research .....	3
1.5 Dissertation layout.....	4
CHAPTER TWO LITERATURE REVIEW .....	5
2.1 Overview .....	5
2.2 Review of different technologies conversion from vibration energy harvesting .....	5
2.3 Summary .....	15
CHAPTER THREE THEORETICAL BACKGROUND ON THE VIBRATION ENERGY HARVESTING.....	17
3.1. Overview of potential ambient energy sources .....	17
3.1.1 Photovoltaic Energy (Solar energy or light energy).....	17

3.1.2 Air flow energy (wind).....	18
3.1.3 Thermal energy.....	19
3.1.4 Vibration energy.....	19
3.1.5 Radio frequency energy.....	20
3.2. Vibration energy harvesting.....	22
3.2.1. Introduction.....	22
3.2.2. Principles of vibration energy harvesting.....	23
3.2.3. Different technologies conversion in vibration energy harvesting.....	26
3.2.3 Summary of different types of conversion technologies.....	38
CHAPTER FOUR PIEZOELECTRIC ENERGY HARVESTING FROM VIBRATION.....	40
4.1 Overview of Piezoelectricity.....	40
4.2 Brief History of piezoelectricity.....	40
4.3 Piezoelectric effect.....	43
4.3.1 Direct piezoelectric effect.....	45
4.3.2 Converse piezoelectric effect.....	46
4.4 Piezoelectric materials.....	47
4.4.1. Modes of piezoelectric materials.....	47
4.4.2. Different types of piezoelectric materials.....	47
4.4.3. Advantages of piezoelectric materials.....	49
CHAPTER FIVE EXPERIMENTAL SETUP AND METHODOLOGY.....	51
5.1 Background.....	51
5.2 Experimental apparatus.....	51
5.2.1. Equipments used.....	52
5.2.2. Piezoelectric material PZT- 4.....	56
5.2.3. Prototype generator.....	58

5.3 Methodology and measurement procedure .....	59
5.3.1. Methodologies .....	59
5.3.2. Measurements procedure .....	61
CHAPTER SIX .....	62
6.1 Description of the prototype generator.....	62
6.2 Basic mode configuration.....	64
6.3 Testing of the prototype generator harvester.....	66
6.3.1. Experimental results and discussion of the prototype generator without tip mass.....	67
6.3.2. Influence of the tip mass on the operation of the energy harvesting.....	69
6.4 Analytical model of prototype generator relating to the influence of the mass .....	71
6.4.1. Geometric terms for piezoelectric cantilever beam .....	71
6.4.2. Dynamic model of piezoelectric cantilever beam .....	75
6.5 Validation of the two approaches to design of the cantilever beam.....	79
CHAPTER SEVEN CONCLUSIONS AND RECOMMENDATIONS .....	82
7.1 Conclusions .....	82
7.2 Recommendations for future work.....	83
REFERENCES.....	85

## LIST OF FIGURES

Figure 3. 1: Inertial vibration energy harvester .....	23
Figure 3. 2: Electromagnetic conversion [49].....	27
Figure 3. 3: Circuit of electromagnetic generator conversion .....	28
Figure 3. 4: Electrostatic conversion [49].....	31
Figure 3. 5: Circuit of electrostatic conversion charge constrained.....	33
Figure 3. 6: Piezoelectric conversion: (a) mode 33 and (b) mode 31 [49] .....	35
Figure 3. 7: Generator circuit piezoelectric conversions .....	36
Figure 4. 1: (a) Mono crystal with single polar axis. (b) Poly crystal with random polar axis. .....	44
Figure 4. 2: Polarization of ceramic material to generate piezoelectric effect. ....	45
Figure 4. 3: (a) Direct piezoelectric effect and (b) Converse piezoelectric effect. ....	45
Figure 5. 1: View of all equipment used.....	52
Figure 5. 2: Electrodynamic vibration exciter shaker .....	53
Figure 5. 3: Amplifier Tira.....	54
Figure 5. 4: Piezoelectric accelerometer model Bruel & Kjaer type 4507 B .....	55
Figure 5. 5: PUMA Vibration Control and Analysis System software.....	56
Figure 5. 6: Picture of the piezoelectric ceramic materials PZT-4. ....	56
Figure 5. 7: Picture of piezoelectric cantilever beam on the shaker .....	58
Figure 5. 8: Schematic diagram of experimental setup .....	60
Figure 6. 1: Piezoelectric cantilever beam without tip mass .....	63
Figure 6. 2: Piezoelectric cantilever beam with tip mass at one end .....	63
Figure 6. 3: Piezoelectric bimorph polarized.....	65
Figure 6. 4: Graph of constant velocity .....	66
Figure 6. 5: Graph showing trends of the voltage output generated across the frequency for the first setup.....	68
Figure 6. 6: Graph showing trends of the voltage output generated across the frequency for the second setup .....	70
Figure 6. 7: Geometry terms of the cantilever beam .....	71

Figure 6. 8: Schematic of piezoelectric bender.....	72
Figure 6. 9: Circuit representation of piezoelectric bimorph.....	75
Figure 6. 10: Time for output voltage for first setup .....	80
Figure 6. 11: Time for output voltage for second setup.....	81

## LIST OF TABLES

Table 3.1: Power density and challenges of typical potential ambient energy sources .....	21
Table 3.2: Electrostatic force variations .....	34
Table 3.3: Summary of different conversion technologies.....	39
Table 4.1: Some properties of common piezoelectric materials .....	49
Table 5.1: Different components of material for PZT-4.....	57

# NOMENCLATURE

## LATIN SYMBOLS

$a$	Acceleration of the vibration [ $\text{m/s}^2$ ].
$B$	Flux density across the coil [T].
$C$	Capacitance between two electrodes [F].
$C_L$	Storage capacity [F].
$C_{max}$	Maximum couple [Nm].
$C_{min}$	Minimum couple [Nm].
$C_{par}$	Parasitic couple [Nm].
$C_V$	Variable capacitor [F].
$D$	Electric displacement in charge per unit area [ $\text{C/m}^2$ ].
$d$	The piezoelectric strain coefficient [ $\text{m/V}$ or $\text{C/N}$ ].
$E$	Electrical field [ $\text{N/C}$ or $\text{V/m}$ ].
$E_A$	Energy of the excitement by cycle vibration [J].
$E_C$	Energy supplied to electric charge [J].
$F$	Axial load positive for a traction load and negative for compressive loads [N].
$F$	Damping force [N].
$F_b$	Axial load required to buckle the beam [N].
$F_{b\ can}$	The buckling load of cantilever [N].
$F_{b\ dcb}$	The buckling load of double clamped beam [N].
$F_{opt}$	Optimum damping force [N].
$f_{ri}'$	Resonant frequency in mode $i$ without load [Hz].
$g$	Gravitational acceleration [ $9,81\ \text{m/s}^2$ ].
$h$	Thickness of the cantilever [m].
$L_C$	Inductance of the coil [H].

$l$	Length of the cantilever and Effective length of the coil [m].
$m$	Seismic mass [g].
$P$	Power [w].
$P_e$	Power load [w].
$R_C$	Resistance of the coil [ $\Omega$ ].
$R_L$	Resistance of the load [ $\Omega$ ].
$R_{opt}$	Optimum value of resistance of the load [ $\Omega$ ].
$S$	Effective area of the coil [ $m^2$ ].
$S$	Strain [m/m].
$S^E$	Compliance when the electric field is constant [ $m^2/N$ ].
$T$	Stress [ $N/m^2$ ].
$t$	Thickness of the piezoelectric material [m].
$V_{in}$	Pre-charged tank [V].
$V_{oc}$	Open circuit voltage [V].
$w$	Width of the cantilever [m].
$Y$	Displacement of the frame [m].
$Y$	Young's modulus of the material of the cantilever [ $N/m^2$ ].

## **DIMENSIONLESS NUMBERS**

$b^*$	Constant linked to the size of the piezoelectric generator.
$b_m$	Parasitic damping coefficient.
$b_e$	Damping coefficient of induced electromagnetic transduction.
$g$	Piezoelectric voltage constant.
$h$	Efficiency of energy conversion.
$k$	Electromechanical coupling coefficient.
$k_a$	Surcharge “negative” spring stiffness.



$k_{eff}$	Effective spring constant.
$k_m$	Mechanical spring constant.
$N$	Number of turns in the coil
$U$	Ratio

## GREEK SYMBOLS

$\varepsilon$	Dielectric displacement per unit electric field and compliance.
$\varepsilon/\varepsilon_0$	Relative permittivity.
$\varepsilon^T$	Dielectric constant (permittivity) under constant stress [F/m].
$\lambda$	Transmission coefficient.
$\lambda_i$	Dimensionless load parameter.
$\eta_A$	Absolute efficiency of energy conversion.
$\zeta_e$	Damping factor electrically induced.
$\zeta_m$	Damping factor mechanically induced.
$\sigma$	Mechanical stress [N/m <sup>2</sup> ].
$\omega$	Angular frequency of vibration [rad.s <sup>-1</sup> ].
$\omega_C$	Angular frequency of cantilever [rad.s <sup>-1</sup> ].
$\omega_r$	Resonant frequency [Hz].

## SUBSCRIPTS

31	Poling direction of the material in mode 1.
33	Poling direction of the material in mode 3.
A	Ambient.
a	Surcharge negative.
b	Buckle the beam.
C	Charge.

can	Cantilever.
dcb	Double clamped beam.
e	Electrically induced.
eff	Effective.
$i$	The $i^{\text{th}}$ normal mode.
in	Inlet.
L	Load.
m	Mechanical.
max	Maximum.
min	Minimum.
oc	Open circuit.
opt	Optimum.
par	Parasitic.
r	Resonant.
v	Variable.

## **SUPERSCRIPTS**

*	Linked to the size.
E	Electric field constant.
T	Constant stress.

## ACRONYMS AND ABBREVIATIONS

DC	Direct Current
e.m.f	Electromotive force.
IEEE	Institute of Electrical Electronic Engineering.
KCL	Kirchhoff's Current Law.
KVL	Kirchhoff's Voltage Law.
MEMS	Micro-Electro-Mechanical System.
MFC	Macro Fiber Composite.
mFupC	Mechanical Frequency up Conversion.
PVDF	Polyvinylidene fluoride or Piezo polymer.
PZT	Lead Zirconate Titanate or Piezo ceramic.
rms	Root-mean-square.
RF	Radio frequency.
SOI	Silicon-on-insulator
QP	Quick Pack.
VIP	Vibration Interactive Program.
VRTC	Vibration Research and Testing Centre.
WSN	Wireless sensor networks.

# CHAPTER ONE

## INTRODUCTION

---

### 1.1 Background

For decades, the concept of energy harvesting has been implemented in energy systems powered by the ambient environment of the real world but its concretization is heavy, complex and expensive. However, examples of markets in which such an energy harvesting approach has been used with success include wireless medical devices, detection of tire pressure, transport infrastructure and building automation [1].

Energy harvesting is defined as a technology that permits the capture of trace amounts of energy from one or more ambient energy sources such as wind, energy of gas, temperature gradients, vibration, liquid flows, etc. and converts it into usable electrical energy. Energy harvesting is the use of ambient energy to deliver electricity for small appliances or mobiles, whether electronic or electrical. It is ideal for wireless sensor and wireless devices networks that rely on rechargeable batteries [2]. This form of energy generation is also called energy scavenging or power harvesting [3].

Several attempts are being made for energy harvesting from the ambient environment in different conversion technologies and their applications. Various environments are subject to ambient vibration energy that is wasted. A variety of conversion technologies exist for converting ambient vibration energy as it exists to a form of mechanical movement that can be harnessed then into electrical energy. The main conversion technologies are electromagnetic conversion, electrostatic conversion and piezoelectric conversion. Ambient vibrations can be found in many applications including natural, commercial, industrial and transport environments. Examples are vehicle engine compartments, ships, bicycles, trains, helicopters, washing machines, fridges, microwave ovens, pumps and machinery, floors (train stations, offices, nightclubs), bridges, walls, window panes, speakers and humans (human heartbeat) [4].

Therefore, vibration energy harvesting is a mechanical process of gathering ambient energy from vibrating source that will be converted to electrical energy using piezoelectric materials. By this approach, the quantity of energy produced is dependent on the amount of the vibration energy obtainable in the environment and the generation efficiency of power conversion [5].

This study focused on piezoelectric conversion, as a process of converting the gathered ambient harvested energy using piezoelectric materials devices as power sources. A good understanding of this conversion of the energy harvesting from vibration using the piezoelectric materials is essential to determine a suitable design methodology, in order to improve the output power that can be used in various domains.

## **1.2 Motivation for this research**

Today, the world is running on electricity. People are relying more on electricity for home lighting in their daily lives, communication entertainment, manufacturing and data processing in business. Low power devices with wireless sensors are emerging for larger applications such as automation, military equipment, environmental monitoring, homeland security and medical equipment, as they offer quite successful power in a compatible size. As these devices are increasing in number and decreasing in size, batteries are no longer a suitable source of energy because of battery size, cost of installation, disposal and replacement. When the battery cannot match the use, the only viable solution to meet electricity needs is produced electricity from renewable energy sources available locally. Energy harvesting is the idea of converting the ambient energy available in the environment to electricity to power local electronic devices. Piezoelectric materials can convert energy associated with mechanical deformation into electrical energy. Such materials have high energy density and electromechanical coupling compared to other technologies energy conversion capability. Vibrations are mechanical energies frequently encountered in the environment with good energy levels. Thus energy from vibration using piezoelectric materials provides an ideal energy solution for portable and wireless devices.

### 1.3 Research questions

For this study to be successful, the fundamental questions that need to be addressed are as follows:

- How can we harvest energy from ambient vibration?
- Which electromechanical structure should be used to harvest mechanical energy by converting it into electrical energy?
- Can this electricity power be used in various domains?

In order to answer the above questions it is necessary to engage in certain prerequisite activities such as a review of related literature, and design of a relevant experiment. In terms of useful prerequisite we shall record different measurements. Experimental skills and a good understanding of vibration energy harvesting by piezoelectric material is needed in order to build up a comprehensive answer that meets the expectations of the study.

### 1.4 Aim and objectives of this research

The aim of this study is to gather ambient energy from vibration sources and convert it into electrical energy using piezoelectric materials. Based upon most considerations raised before, the objectives of this project are thus to:

- Develop a prototype generator with piezoelectric materials to predict the performances of harvesting vibration energy. This prototype generator will be used for various measuring (voltage, power, frequency, etc.) and to convert the mechanical energy into electrical energy from vibration source.
- Establish an experimental procedure to collect data and analyze the results obtained from experimental measurement.
- Validate the prototype generator and determine the effect of the mass, the geometric dimensions and the choice of materials, on energy harvesting.

## 1.5 Dissertation layout

The dissertation is structured into the following seven chapters:

Chapter One introduces the study and the research questions to be answered and the aim and objectives of the study.

Chapter Two presents the literature review of previous research work in the area of energy harvesting by vibration.

Chapter Three provides background on vibration energy harvesting from different environmental sources using different conversions technologies.

Chapter Four presents the theories of piezoelectricity and its history. The different materials used and their behaviors are summarized.

In Chapter Five, the experimental setup and methodologies used in this study are presented.

Chapter Six presents the experimental results from the experiment. The achieved results are analyzed and discussed by determining the impact of the variation of main parameters of the prototype on the output energy.

In Chapter Seven, the main conclusions of this study are summarized. Based on the results obtained, recommendations are given for future work in the area of energy harvesting by vibration from this study.

# CHAPTER TWO

## LITERATURE REVIEW

---

### 2.1 Overview

The scientific literature has recently shown a significant increase in the number of articles describing research in the field of energy harvesting. Various aspects of energy harvesting have been studied by different researchers, in particular from vibration, to develop and understand power harvesting systems with importance placed on the different technologies used to harness electricity from vibrations. The biggest challenge was to generate useful electricity for consumption and increase performance of recovery. The literature review presented in this chapter will provide a review of recent studies that allowed advancement of knowledge in vibration energy harvesting.

### 2.2 Review of different technologies conversion from vibration energy harvesting

There are several different technologies to convert energy from mechanical vibration to electrical energy. The main conversion technologies are electromagnetic conversion, electrostatic conversion and piezoelectric conversion. In this literature review, we will start with some studies in electromagnetic conversion, electrostatic conversion and finish with piezoelectric conversion where the studies show the possibility of making use of piezoelectric materials as sources of power.

Beeby et al. [6] studied energy harvesting by placing a coil at the end of a cantilever overhang excited by the base and oscillating between two magnets. They presented a small volume electromagnetic generator (component volume  $0.1 \text{ cm}^3$ , practical volume  $0.15 \text{ cm}^3$ ) optimised for harvesting by vibration from low level ambient vibration based on real application data. The generator produced useful power of  $46 \text{ }\mu\text{W}$  to a resistive load of  $4 \text{ k}\Omega$  from a vibration level of  $60 \text{ mg}$  ( $g = 9.81 \text{ m/s}^2$ ), when the electromagnetic device was shaken at a resonant frequency of  $52 \text{ Hz}$ . The generator delivered  $30 \%$  of the total power dissipated in the generator to electrical power in the load. From the basic equations governing



electromagnetic generators, they concluded that the energy decreases with device volume, and reducing input vibration acceleration.

Li et al. [7] developed a vibration harvesting power generator with a total volume of  $1 \text{ cm}^3$  using a laser micro machined resonant copper spring based on Faraday's Law of induction according to which a spring can convert mechanical energy into useful electrical power. Using innovative designs, the mass can be vibrated horizontally while the vibration input is applied vertically. The substantially horizontal vibration provides the highest output voltage of the generator. Li et al. developed a generator capable of producing a voltage of 2 V DC with 64 Hz to 120 Hz input frequency at 250 to 100  $\mu\text{m}$  vibration amplitude.

Williams et al. [8] developed a design methodology for linear micro-generators, where the design was applied to a millimetre scale microwave electromagnetic generator. The manufacture of a prototype device is described using generally available micro fabrication techniques. The results of the testing of the device in relation to a source of variable amplitude vibrations, in a vacuum and in air, are presented. With the device prototype, the electric power generation from mechanical vibration power was  $0.3 \mu\text{W}$  at an excitation frequency of 4 MHz. The energy generated by such devices is proportional to the mass and vibration acceleration and inversely proportional to resonant frequency as well as mechanical (electrical) damping factor. This means that more power can be extracted if the inertial mass is increased or the generator can work in the environment where the vibration level is high. To maximize the power that may be produced in any particular application, the resonant frequency of the generator must be designed to match the frequency range of the vibration source, and the maximum possible deformation of the device should be as great as possible. They concluded that mechanical damping is a dominant limiting factor in these devices and significant improvements in the output power can be achieved through better linearity of the spring and the load operation. Electromagnetic coupling also needs to be optimized to ensure a good impedance match between the device and the electric load.

Zhang and Kim [9] described a new idea to increase the energy conversion efficiency of electromagnetic transduction by orders of magnitude. They used an array of alternating north- and south-orientation magnets to enhance magnetic flux change by more than an order of

magnitude. Magnetic flux changes for a magnet array and a single magnet are simulated and compared. A micro fabricated energy harvester of  $20 \times 5 \times 0.9$  mm weighing 0.5 g generates an induced electromotive force of  $V_{p-p} = 30$  mV with 2.6  $\mu$ W power output into 10.8  $\Omega$  load when it is vibrated at 290 Hz with a vibration amplitude of 11  $\mu$ m. The macro scale version, scaled up to  $51 \times 51 \times 10$  mm weighing 90 g, generates an induced electromotive force of  $V_{p-p} = 22$  V with 158 mW power output (into 96  $\Omega$  load) when it is vibrated at 82 Hz with a vibration amplitude of 414  $\mu$ m, and lights an incandescent light bulb.

Zorlu and Klah [10] presented a collector of electromagnetic energy from non-resonant Micro-Electro-Mechanical System (MEMS) based environmental vibration, which generates energy from low frequency vibration with a small amplitude movement. They used a prototype electromagnetic transduction technique to produce electrical energy. This type of technique can be adapted also for electrostatic and piezoelectric conversion. The size of the prototype was  $4 \times 8.5$  mm, and the peak to peak of the magnet movement was between 3 to 5 mm. It generated an *rms* power of 18.5  $\mu$ W and *rms* voltage of 2.1 mV at a frequency of 10 Hz, with external vibration of 5 mm peak to peak (1 g) and energy of 1.1  $\mu$ J which was transferred to equivalent resistive loads of each coil per occurrence of the mechanical frequency up conversion (mFupC). This prototype is a good candidate for application of energy harvesting with characteristics of non-resonant vibration, including human movement, the movement of branches of trees and the movements of a vehicle.

Wang et al. [11] designed, simulated, fabricated and characterized a micro electromagnetic vibration energy harvester with sandwiched structure and air channel. The harvester consists of the lower coil, an upper coil, an NdFeB permanent magnet and a plane of nickel with the spring integrated frame of silicon. The natural frequency of the magnet-spring system tested is 228.2 Hz. Comparison of the natural results tested and simulation shows that the micro electroplated Ni film Young's modulus is about 163 GPa rather than 210 GPa of bulk Ni material. These experimental results show that the air channel in the silicone frame of the prototype and the sandwiched structure are able to increase the induced voltage to 42 % of the single coil. The prototype has a resonant frequency of 280.1 Hz at an acceleration of 8  $\text{m/s}^2$  which results from the nonlinear magnet-spring system. The prototype at resonant frequency of 280.1 Hz and 8  $\text{m/s}^2$  input vibration acceleration generated 162.5 mV charging

voltage. The maximum charging power obtained was approximately 21.2  $\mu\text{W}$  corresponding to 66.25  $\mu\text{W}/\text{cm}^3$  when the optimum load resistance was 81  $\Omega$ .

Chiu et al. [12] analysed and modelled the nonlinear dynamics of a DC battery-charged vibration-to-electricity energy converter. The maximum output power and optimal design under restricted area and voltage were found by resolving the nonlinear equations of movement. To allow the integration with power management circuits, the output voltage is limited to 40 V. Under these conditions, the maximum power was 38.1  $\mu\text{W}$  and 0.87  $\mu\text{W}$  for a device with and without a 4 gr external mass, respectively. The authors concluded that the optimized converters can produce significant power only for a limited range of design and operation parameters. Over certain range of these parameters, the converters could not operate stably.

Paracha et al. [13] experimentally demonstrated the ability to scavenge the energy of mechanical vibration energy to provide electrical energy to a resistive load by using an electrostatic silicon-based MEMS transducer manufactured in CMOS-compatible technology. Paracha et al. found that the converted power was between 60  $\mu\text{W}$  and 100  $\mu\text{W}$ , for an external vibration of 250 Hz as resonant frequency and amplitude of acceleration of 0.25  $g$  where  $g$  is gravitational acceleration 9,81  $\text{m}/\text{s}^2$ . They proposed a novel method for calculating the maximum power that can be produced from a spring-mass system excited with a sinusoidal force, based on the analogy of an electrical impedance network.

Lee et al. [14] provided a comparison of the capabilities of harvesting energy from three different electrostatic mechanisms and discussed the relationship between the parameters that contribute to maximizing the energy that can be harvested from a micro electro mechanical electrostatic system (MEMS) apparatus. The three mechanisms considered were: the plane-overlap, in plane gap closing and out-of-plane gap closing. Based on the analytical model, the mass of the moving loads and cross-sectional surfaces of the devices active regions were set to be the same for all devices, while assuming that the electrostatic mechanisms operated in an ideal vacuum environment. Some case studies have shown that an in-plane gap closing structure has the potential to produce a higher amount of energy per unit volume compared to

an out-of-plane gap closing mechanism provided that the thickness of the mass of the structure the in plane gap is above the critical value.

Cottone et al. [15] developed a novel vibration energy harvester design consisting of a double-mass contactless frequency-up converter with buckled clamped-clamped beams aimed at increasing energy harvesting efficiency from low-frequency vibrations. This concept aims at increasing the energy harvesting efficiency for low frequency vibrations. The mechanical to electrical energy conversion was performed through a silicon MEMS micro electrostatic generator based on interdigitated combs. A device prototype was fabricated and experimentally investigated under harmonic frequency sweeping at 0.2 g rms ( $g = 9.81 \text{ m/s}^2$ ) and band-limited colored noise 0.15 g rms with a precharge voltage of 2.5 V. In the buckled-beam bistable configuration, the researchers found that the electrostatic generator showed a gain factor of 100 % that mean the harvested power increases of more than 100 times at low frequencies in the interval vibrations between 20 and 50 Hz for the bistable mode versus the normal operation mode, despite of the fact that the converter itself was designed to resonate at 162 Hz. Cottone et al. claim that this concept can be applied to different transduction techniques.

Kempitiya et al. [16] proposed a technique to improve the output power from vibration-based charge-constrained electrostatic ambient energy harvesters. Converting synchronous energy to produce a net energy gain with minimum power dissipation without the need for complex sensing mechanisms is a contribution of the proposed control technique. The energy harvesting circuit produces a measured power of 1.688  $\mu\text{W}$  for a power investment of 417 nW. The measured power consumption associated with the on-chip controller unit is 24 nW, approximately 1.42 % of the total power harvested. According to Kempitiya et al., this type of micro-watt power generation circuit can be considered for powering communications transceivers and portable electronic devices.

Galayko et al. [17] investigated the dynamic behaviour of an electrostatic Energy Vibration Harvester (e-HEV) which uses gap-closing capacitive sensors operating in a constant charge mode. The authors studied theoretical insight allowing a quantitative characterization of the highlighted instability phenomena and found that, depending on the amplitude of the external

vibrations, three types of pathological behaviour occur at low amplitude, large amplitude and middle amplitude. The study showed that none of this behaviour was similar to that observed for a constant voltage biased capacitive transducer.

Chiu et al. [18] designed and analysed a micro vibration-to-electricity converter. In design, the output power was  $200 \mu\text{W}/\text{cm}^2$  of chip area constraints for optimal load of  $8 \text{ M}\Omega$ . The device was manufactured in a silicon-on-insulator (SOI) wafer, and electrical and mechanical measurements were made. Impedance measurements showed undesirable parasitic conductance leading to the failure of the measurement of the output power.

Chen et al. [19] have modelled a new cantilever piezoelectric bimorph transducer converting micro electro-mechanical energy, based on the basic approach. The analysis model showed that the voltage induced by vibration was proportional to the excitation frequency of the device, but inversely proportional to the length of the cantilever beam and the damping factor. Chen et al.'s experimental results indicated that the maximum output voltage differed very slightly from the energy conversion analytical model..

Lu et al. [20] proposed a new maximum power point (MPP) tracking system to harvest the maximum power from a vibration system. An energy harvesting system based on vibrations and piezoelectric conversion for micro power supply was made and presented. The circuit was fabricated and measurements were carried out to verify the tracking performance and the feasibility of the proposed platform. The results showed that the power harvesting efficiency of the overall circuit was over 90 %.

Elvin et al. [21] developed a novel damage detection sensor which was self-powered and was also able to transmit information wirelessly to a remote receiver. Sensor performance was illustrated by means of theoretical and experimental analysis of a simple damaged beam. Their results showed that a sensor powered from the conversion of mechanical energy into electrical energy is viable for damage detection. The potential benefits of this sensor include ease structure implementation during manufacture and the use of an environmentally safe renewable power source.

Sodano et al. [22] developed a model of the piezoelectric power harvesting device. The derivation of the model has been provided, allowing it to be applied to a beam with various boundary conditions or layout of piezoelectric patches. The model was verified using experimental results and proved to be accurate independent of the precise frequency of excitation and the load resistance. The measured current generated by the Quick Pack was compared to the predicted current from the model for various frequencies and load resistances. The verification of the model was performed on a structure the contained a complex piezoelectric layout and a non-homogenous material beam, indicating that the model is robust and can be applied to a variety of different mechanical conditions. The damping effects of power harvesting were also shown to be predicted in the model and to follow that of a resistive shunt damping circuit.

Qiu et al. [23] introduced research activities of vibration control and energy harvesting using piezoelectric materials and a nonlinear approach based on Synchronized Switch Damping (SSD). The SSD technique, also called pulse-switched method, consists in a nonlinear processing of the voltage on a piezoelectric actuator. It is implemented with a simple electronic switch synchronously driven with the structural motion. This switch, which is used to cancel or inverse the voltage on the piezoelectric material, allows to briefly connecting a simple electrical network (short circuit, inductor, voltage sources depending on the SSD version) to the piezoelectric material. Due to this process, a voltage magnification is obtained and a phase shift appears between the strain in piezoelectric patch and the resulting voltage. The force generated by the resulting voltage is always opposite to the velocity of the structure, thus creating net mechanical energy dissipation. The dissipated energy corresponds to the part of the mechanical energy which is converted into electric energy. Maximizing this energy is equivalent to minimizing the mechanical energy in the structure under given excitation. This process increases the amount of converted electrical energy during a mechanical loading cycle of the piezoelectric material.

Roundy et al. [24] had developed a composite piezoelectric cantilever beam generator . The cantilever used was of constant width which simplifies the analytical model and beam fabrication but results in an unequal distribution of strain along its length. A prototype generator was fabricated by attaching a PZT-5A shim to each side of a steel centre beam. A

cubic mass made from an alloy of tin and bismuth was attached to the end and the generator tuned to resonate at 120 Hz. The prototype produced a maximum power output of nearly 80  $\mu\text{W}$  into a 250 k $\Omega$  load resistance with 2.5  $\text{m.s}^{-2}$  input acceleration and the results showed a reasonable level of agreement with the analytical models. These models were then used to optimize the generator design within an overall size constraint of 1  $\text{cm}^3$ . Two designs were adopted, each using PZT-5H attached to a 0.1 mm thick central brass shim. Design 2 using a PZT thickness of 0.28 mm, possessing a beam length of 11 mm and a tungsten proof mass of  $17 \times 7.7 \times 3.6$  mm, produced 375  $\mu\text{W}$  with an input acceleration of 2.5  $\text{m.s}^{-2}$  at 120 Hz. This generator was demonstrated powering a radio transceiver with a capacitor used for energy storage and achieved a duty cycle of 1.6%. Roundy et al. concluded that the generator output at resonance is proportional to the mass attached to the cantilever and this should be maximized provided size and strain constraints are not exceeded.

Leland and Wright [25] changed the natural frequency range of a piezoelectric bimorph by applying axial compression to lower its resonance frequency. In this way, they were able to reduce the frequency of resonance by 24% below its original value while maintaining a relatively constant dissipated power despite an increase in the rate of mechanical damping. The prototype developed was produced 300 – 400  $\mu\text{W}$  of power at driving frequencies between 200 and 250 Hz. Additionally, piezoelectric coupling coefficient values were increased using this method, with  $k_{\text{eff}}$  values rising as much as 25% from 0.37 to 0.46.

Eichhorn et al. [26] proposed a piezoelectric energy converter in which application of effort tension or compression to the collector increased the frequency band of where recovery was effective. The converter consisted of a piezo-polymer cantilever beam with two additional thin arms, which were used to apply an axial preload to the tip of the beam. This design allowed lessening of the resonance frequency of a harvester by applying compression loading could be altered from 380 Hz to 292 Hz and a harvester with stiffened arms was tuned from 440 Hz to 460 Hz by applying a tensile preload. In combination with the automatic control of the applied force, this type of structure could be used to improve the performance of energy harvesters in vibrating environments with occasional changes in the vibration frequency

Challa et al. [27] proposed the design and testing of a resonance frequency tunable energy harvesting device using a magnetic force. The technique was about to place a pair of magnets at the end of the collector and another on a case surrounding the recovery. Positions of the magnets are chosen so that an attraction force and repulsion force is applied on the collector thus inducing a magnetic stiffness. To control the frequency of resonance of the collector, the distances between pairs of magnets can be adjusted and so decrease or increase the magnetic stiffness. This technique enabled resonance tuning to  $\pm 20\%$  of the untuned resonant frequency. In particular, this magnetic-based approach enabled either an increase or decrease in the tuned resonant frequency. A piezoelectric cantilever beam with a natural frequency of 26 Hz was used as the energy harvesting cantilever, which was successfully tuned over a frequency range of 22–32 Hz to enable a continuous power output 240 – 280  $\mu\text{W}$  over the entire frequency range tested.

Roundy et al. [28] analyzed and made a piezoelectric bimorph (PZT) generator with a central steel shim. The cantilever structure had an attached mass. The volume of the total structure was  $1 \text{ cm}^3$ . A model of the piezoelectric generator to the point was made and validated. For a vibration input of approximately  $2.25 \text{ m/s}^2$  at 120 Hz, a power of 125 mW to 975 mW was produced, depending on the generated load. Power recovered was analyzed directly connecting the generator to a resistive load or a capacitive load. Later, a DC-DC converter was included and the generator power was supplied to a low power transceiver. The radio transmitted at 1.9 GHz and consumed 10 mA at 1.2 V and the source of vibration was  $2.25 \text{ m/s}^2$  at 60 Hz

Peters et al. [29] presented an electrically tunable resonator which can be used as a resonator structure for recovering the energy of vibration. The adjustment of the resonance frequency is provided by the mechanically reinforcing the structure using piezoelectric actuators. The authors used two piezoelectric actuators together, the one free and the other clamp. The application of an electrical potential to the two actuators increased the rigidity of the structure. Therefore, the natural frequency of the mass-spring system of rotation increased. The control voltage was chosen to be  $\pm 5 \text{ V}$  leading to a change of initial resonance measured at 15 Hz around the resonance frequency of 78 Hz.



Fang et al. [30] fabricated a MEMS-based PZT cantilever power generator with a non-integrated Ni proof mass that could generate  $2.16 \mu\text{W}$  from  $10 \text{ m/s}^2$  vibration acceleration at its resonant frequency of 609 Hz. The nickel metal mass on the tip of the cantilever was used to decrease the structure's resonant frequency for the application under low-frequency vibration, but it could not be micro-machined by MEMS technology.

Similar to the previous work, Liu et al. [31] used the previous cantilever structure to construct a power generator array to improve power output and frequency flexibility. The prototype generator has a measured performance of  $3.98 \mu\text{W}$  of effective electrical power and 3.93 DC output voltage. Although they demonstrated that power density was high, the proof mass could also not be integrated with the cantilever which would be an additional difficulty in production. This device is promising to support networks of ultra-low-power, peer-to-peer, wireless nodes..

Renaud et al. [32] proposed a fabricated MEMS-based PZT cantilever micro-generator with an integrated proof mass that can generate an average power of  $40 \mu\text{W}$  at 1.8 kHz vibration frequency. The model indicates that the frequency of the input vibration leading to the maximum output power is not always equal to the short circuit natural frequency of the bender. The theoretical results for the output power obtained in the framework of this approximation were consistent with experimental results.

Muralt et al. [33] designed and fabricated a micro power generator of thin film PZT laminated cantilever with proof mass and interdigitated electrodes which could generate a voltage of 1.6 V and power of  $1.4 \mu\text{W}$  when excited at less than  $20 \text{ m/s}^2$  vibration acceleration at 870 Hz resonant frequency.

Zhou et al. [34] proposed and investigated a novel piezoelectric energy harvester with a multimode dynamic magnifier capable of significantly increasing the bandwidth and the energy harvested from ambient vibration. The design comprised a multimode intermediate beam with a tip mass, called a dynamic magnifier and an energy harvesting beam with a tip mass. The theoretical analysis is conducted for the coupled beams by considering the interaction of one beam with the other. From the mode shapes of the first six resonant frequencies of the coupled structure drawn from the theoretical and finite element modelling

(FEM) analyses, it is shown that the voltage generated by the energy harvesting beam is dramatically magnified in a broad bandwidth and the vibration of the primary beam is mitigated. Zhou et al. experimentally demonstrated that 25.5 times more energy can be harvested in a frequency range of 3 – 300 Hz from the energy harvesting beam by adding a multi-mode dynamic magnifier. The energy harvesting is increased by 100 – 1000 times near these resonances of the harvesting beam.

Patel et al. [35] proposed a versatile model for optimizing the performance of a rectangular cantilever beam piezoelectric energy harvester used to convert ambient vibrations into electrical energy. The developed model accounts for geometric changes to the natural frequencies, mode shapes, and damping in the structure. This is achieved through the combination of finite element modelling and a distributed parameter electromechanical model, including load resistor and charging capacitor models. The model has the potential for use in investigating the influence of numerous geometric changes on harvester performance, and incorporates a model for accounting for changes in damping as the geometry changes. The model is used to investigate the effects of substrate and piezoelectric layer length, and piezoelectric layer thickness on the performance of a microscale device. Findings from a parameter study indicate the existence of an optimum sample length due to increased mechanical damping for long beams and improved power output using thicker piezoelectric layers. To achieve unbiased comparisons between different harvester designs, parameter studies are performed by changing multiple parameters simultaneously with the natural frequency held fixed. Performance enhancements were observed using shorter piezoelectric layers as compared to the conventional design, in which the piezoelectric layer and substrate are of equal length.

### 2.3 Summary

The literature review has shown several methods for electromechanical vibration-to-electricity conversion. The commonest method employed to characterize an energy harvesting by vibration is to excite the energy harvester under a sinusoidal vibration at its resonant frequency and to measure the output voltage across the structure. This is the most straight forward way of evaluating output power of a vibration energy harvester. However, in

practical application, the vibration spectrum usually contains more than one peak at different frequencies. It is important to understand whether other frequencies will affect the vibration energy harvesting work at one particular frequency. Even so, it has been demonstrated by many different researchers that using piezoelectric materials as conversion mechanisms is an effective design to provide sufficient electrical power for micro-electromechanical systems (MEMS) and vibration energy harvesting using piezoelectric materials under practical vibration are viable.

## CHAPTER THREE

# THEORETICAL BACKGROUND OF ENERGY HARVESTING BY VIBRATION

---

This chapter starts with an overview of different potential ambient energy harvesting source finding in the ambient environment and will finish by different technologies of vibration energy harvesting existing to convert ambient energy in the form of mechanical to electrical energy and will also give their advantages and disadvantages.

### 3.1. Overview of potential ambient energy sources

There is a large amount of energy in the ambient environment. The most common are solar energy (light energy) derived from artificial or natural sources, air flow energy in the form of the wind from artificial or natural sources, thermal energy which is inherent within a temperature gradient, kinetic energy in the form of vibration where a device can collect the vibrations when it is situated on structural components of machines or other places close to vibration sources, and Radio Frequency (RF) radiation from artificial or natural sources. By definition, energy harvesting is a process which constitutes to capture a portion of the energy from the ambient environment and to convert it into usable electrical energy. The density of these energy sources is lower than fossil fuel and nuclear fuel. To ensure a reliable source of energy, it is possible to excerpt energy from the ambient environment and store it in a battery.

#### 3.1.1 Photovoltaic Energy (Solar energy or light energy)

Photovoltaic energy is harvested from ambient light or sunlight through solar panels or photo sensors. Solar or light energies can be converted into electrical power using solar cells, which are commercially mature and well characterized. The amount of energy generated varies from  $15 \text{ mW/cm}^2$  from noon-time sun and  $10 \text{ }\mu\text{W/cm}^2$  from indoor incandescent lighting. The conversion of solar energy into electricity has so far focused on two approaches [36]. The first one is solar cell also called photoelectric cell or photovoltaic cell. Here, the

device directly converts the solar or light energy into electricity via the photovoltaic cell (photoelectric). The second is solar-thermal that converts solar or light energy into thermal and uses mechanical heat engines to generate electricity [37]. Solar-thermal achieve about 5 % maximal conversion efficiency [38], which is much lower than the conversion efficiency of solar cell. A solar cell usually converts 17 % of solar energy into electricity, this value can reach 35.8 % the laboratory [39].

In circuit design, the standard solar cell can be modelled as a voltage source in series with an internal resistor. A particular solar cell consists of an open circuit voltage of 0.6 V, but panels with series and parallel combinations of such cells can generate any required voltage for circuit. Although the output voltage is fairly constant in the rated range, the current varies with light intensity. Solar power is more expensive than conventional methods. In addition, daily temperature changes cause irregularity in the quantity of irradiation reaching the ground. The change in the amount of solar or light energy that reaches the ground due to seasonal impact and daily temperature variability makes dependable solar power practically impossible in many geographical locations.

### **3.1.2 Air flow energy (wind)**

Air flow (wind) in the atmosphere is a result of pressure differences caused by the sun heating up different parts of the atmosphere. Almost 2 % of solar energy that reaches the earth is converted into wind energy [40]. Humans have used wind as a power source for thousands of years: for propelling ships and boats by use of a sail, and for milling grain through the use of windmills. On a smaller scale air flow is readily available in a variety of environments, including ventilating and air conditioning ducts, convection from heating sources, and on moving vehicles. Figures stated in the literature for typical air velocities in these environments include: “12 m/s in large ducts, down to 1-2 m/s close to the exit in rooms” [41], 10 m/s (for which the source specifies a power level of  $256 \mu\text{W}/\text{cm}^2$  may theoretically be possible), and 6.1 m/s in an air conditioning duct [42]. The energy harvesting potential of the flow rate in an air conditioning duct “ moving at a velocity of 6.1 m/s through an area of one square centimetre is 12.4 mW ” [43].

### 3.1.3 Thermal energy

Thermal energy is captured from human skin, furnaces, vehicle exhausts, domestic radiators and friction sources. The thermal energy (temperature gradients) in the ambient environment can be directly converted to electrical energy via the thermoelectric effect or the Seebeck effect [44]. A temperature difference between two points in conductor or semiconductor materials results in heat flow and consequently charge flow. *Vice versa*, when a current is made to flow through a junction composed of two materials (A and B), the heat generates at one side and absorbs at the other side. In brief, the power and voltage produced is proportional to the Seebeck coefficient from the thermo-electric materials and the difference in temperature. Large temperature gradients are necessary to produce practical power and voltage levels. However, differences in temperature above 10° C are scarce in a microsystem thus producing low voltage and power levels.

### 3.1.4 Vibration energy

Vibrations are available in many environments of interest including commercial buildings, bridges, highways, aircrafts, helicopters, ships, trains, floors (train stations, offices, nightclubs), industrial facilities, car engine compartments, household appliances (washing machines, fridges, microwave ovens), floors (nightclubs, train stations, offices), walls, window panes, speakers, motors, compressors, pumps, chillers, conveyors, etc. [24]. Vibration source could generate about 300-800  $\mu\text{W}/\text{cm}^3$  in such environments [45]. The conversion of vibrations in the ambient environment to electricity is a potential energy source to supply self-sustaining wireless sensor networks. In general, frequency and acceleration are the key parameters to assess vibration sources. The higher those values, the larger the provided power is to energy harvesters. Most civil vibration sources such as microwave ovens, kitchen blenders and truck engines have a low frequency vibration up to 150 Hz and their acceleration is usually less than 0.5 g where  $1 \text{ g} = 9.81 \text{ m/s}^2$ , the gravitational acceleration. For long-span bridges, the frequency and acceleration become even lower at  $< 0.1 \text{ Hz}$  and  $0.0001 \sim 0.1 \text{ g}$ , respectively. On the contrary, there are significant ambient vibrations available in aerospace structures - up to 1 g between 300 Hz to 1 kHz.

### 3.1.5 Radio frequency energy

A further potential way to power wireless sensor networks (WSN) is the transmission of wireless energy by electromagnetic waves as RF radiation. This notion uses two dissimilar RF sources of energy which are ambient environment RF radiation and controlled RF sources like high power line emissions, infrared, microwaves and cell phones. It has been shown that electronics could effectively capture the ambient RF radiation and then convert it into expedient electricity. With this approach, only electronics with very low power consumption can be driven but the amount of harvested power required is minimal, characteristically within the range of microwatt ( $\mu\text{W}$ ).

Consequently the technique which has had the most attention is controlled RF sources. One approach of controlled RF sources is based on RF links which consists of primary and secondary coils. When the two coils are close to each other and well centre-aligned, the input AC power can be wirelessly transferred from primary coil to secondary coil via the inductive link. Another controlled microwave transmission, so called beamed RF source, also holds promise. An antenna which serves as a source is made to convey microwaves through ambient air to a receiver, and this in turn transforms the microwaves into DC power. The usage of antenna as receivers have achieved the efficiencies in the 50 % - 80 % range for DC to DC conversion.

Different ambient energy sources were compared. Table 3.1 illustrates some sources of the potential ambient energy harvesting with their corresponding power generation capability and some of the current challenges [46].

**Table 3.1: Power density and challenges of typical potential ambient energy sources [46]**

Energy source	Characteristics	Power density	Efficiency	Challenges
<b>Solar or Light</b>	Outdoor	100 mW/cm <sup>3</sup>	10 - 25 %	As solar energy harvesting is an established technology, looking at small-scale harvesters is a challenge due to the fact that power output is directly linked to surface area. For design of embedded wireless sensor nodes to be positioned indoors or in areas such as buildings, and forestry terrains, where contact with direct sunlight is seldom available, solar energy source may not be feasible.
	Indoor	100 μW/cm <sup>3</sup>		
<b>Thermal</b>	Human	60 μW/cm <sup>3</sup>	0.1 - 3 %	An electric current is produced when there is a temperature difference between two joints of a conducting material. Thermal energy harvesting utilizes temperature gradients to generate electricity. Efficiency of conversion is limited by the Carnot cycle. The efficiency of thermo-electric generators is typically less than 1% for temperature gradient less than 40° C while it is difficult to find such temperature gap in the ambient environment.
	Industrial	10 mW/cm <sup>3</sup>		
<b>Vibration</b>	Hz - human	4 μW/cm <sup>3</sup>	25 - 50%	Energy from vibrations can be harnessed by employing suitable mechanical-to-electrical energy converter. Generators generally use electromagnetic, electrostatic, or piezoelectric principles. Vibration energy harvesting is therefore dependent on excitation of the power tends to be proportional to the driving frequency and the input displacement.
	KHz - machines	800 μW/cm <sup>3</sup>		
<b>Radio frequency</b>	GSM 900 MHz	0.1 μW/cm <sup>3</sup>	50 %	Without a dedicated radiating source, ambient levels are very low and are spread over a wide spectrum. There is a limit to the amount of power available for harvesting since the IEEE 802.11 standard prescribes the maximum allowable transmission power (1000 mW in the USA, 100 mW in Europe, and 10 mW/MHz in Japan).
	Wi-Fi 2.4 GHz	0.001 μW/cm <sup>3</sup>		



From Table 3.1, we can be seen that mechanical vibrations can be potentially outperformed by solar energy because of the high energy density insufficiency. However, a solar energy source cannot be a good option when the wireless sensor nodes are situated in areas like inside buildings or forest land in which access to direct sunlight is unavailable. Furthermore, vibration is an interesting option because it is one of the major common energy sources and represents a large part of the mechanical energy source available in the ambient environment. They can be converted into electrical energy through electromagnetic, electrostatic and piezoelectric conversions. Among the three conversion mechanisms, the piezoelectric conversion has the advantages of low mechanical damping, high electromechanical coupling, appropriate voltage and current output and compatibility with MEMS processes. Thus, the focus of this dissertation is the energy harvesting from vibration through piezoelectric conversion. The energy sources of mechanical vibrations are easily accessible by MEMS technology and they are applicable at the macro and micro scale [4] [47] [48].

## **3.2. Vibration energy harvesting**

### **3.2.1. Introduction**

Vibration energy represents the most abundant energy source after solar energy. Vibration energy harvesting is a mechanical process of gathering ambient energy from a vibration source and converting it into electrical energy. The techniques or technologies used to recover the energy produced in the environment by vibrations are arousing more and more interest and these can be converted into energy production tools. The exploitation of ambient vibration energy appears to be an excellent way of converting vibration energy into electricity. Vibration energy harvesting is converted into electrical energy through various techniques, including: Electromagnetic conversion which implements the inductive effect, Electrostatic conversion based on the electrical force generated among two plaques of one charged capacitor and Piezoelectric conversion which converts a mechanical stress into electrical charges directly [5]. In the following sections, these different types of conversion techniques are described and examined.

### 3.2.2. Principles of vibration energy harvesting

Inertial based vibration energy harvesters are modelled as second-order, spring-mass systems. The generic model of principles operation of vibration energy harvesters were proposed by Williams and Yates [49]. Transducers consists of seismic mass  $m$  attached to housing by spring constant  $k$  as shown in Figure 3.1. Damping element represents both damping of spring and damping due to conversion of mechanical energy into electrical energy. When generator is vibrated, inertial mass moves out of phase with movement of the generator housing. Relative motion between seismic mass and generator housing can drive suitable transducer to generate electrical energy. Since the generator is inertial device, it only needs to be fixed to vibrating structure at one point [49]. The damping coefficient  $b$  consists of mechanically induced damping (parasitic damping) coefficient  $b_m$  and electrically induced damping coefficient  $b_e$ , may be expressed as  $b = b_m + b_e$  [50].  $y(t)$  is the displacement of the generator housing and  $z(t)$  is the relative motion of the mass with respect to the housing. For a sinusoidal excitation,  $y(t)$  can be written as  $y(t) = Y \sin \omega t$ , where  $Y$  is the amplitude of vibration and  $\omega$  is the angular frequency of vibration [50].

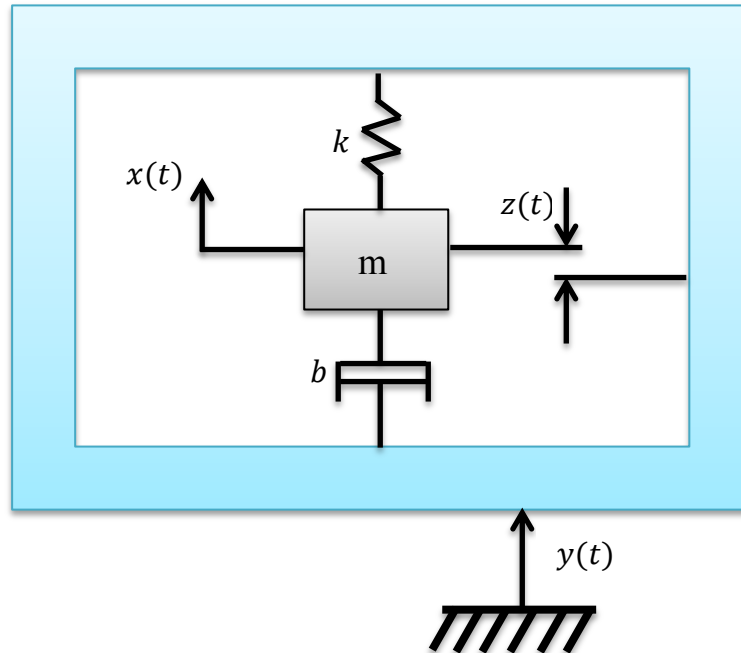


Figure 3. 1: Inertial vibration energy harvester

The means of energy extraction may consist of magnetic seismic mass moving past a coil for electromagnetic energy harvesting, variable capacitor plates mounted on spring for electrostatic harvester and beam made of piezoelectric material for piezoelectric harvester.

For the analysis, it is assumed that the mass of the vibration source is much greater than the mass of seismic mass in the generator and the vibration source is unaffected by the movement of the generator. For linear spring and damping elements, equation of motion of inertial harvester is:

$$m\dot{z} + b\ddot{z} + kz = m\ddot{y} \quad 3.1$$

Considering harmonic excitation  $y = Y \sin(\omega t)$ , equation 3.1 will be:

$$m\dot{z} + b\ddot{z} + kz = m\omega^2 Y \sin(\omega t) \quad 3.2$$

Multiplying equation 3.2 by  $\dot{z} = \dot{x} - \dot{y}$  and rearranging, we get expression:

$$\frac{dy}{dt} \left( \frac{m\dot{x}^2}{2} + \frac{kx^2}{2} \right) + b\dot{z}^2 + (b\dot{z} + kz)\dot{y} = 0 \quad 3.3$$

Where the first member represents the time rate of increase of kinetic and strain energies, second member represents power dissipated by damping and third member of the equation is the instantaneous power into the system.

Assume that the input is a sinusoid excitation, steady-state solution of equation 3.2 is given by:

$$z = Z \sin(\omega t + \varphi) \quad 3.4$$

$$Z = \frac{m\omega^2 Y}{\sqrt{(k - m\omega^2)^2 - b^2\omega^2}} \quad 3.5$$

where  $\varphi$  is the phase angle and given by  $\varphi = \tan^{-1} \left( \frac{b\omega}{k - \omega^2 m} \right)$

The average power out of the generator dissipated within the damper, i.e. the sum of the power extracted by the transduction mechanism and the power lost in mechanical damping is given by:

$$P_{AV} = \frac{bm^2\omega_n^6Y^2}{2[(k - m\omega^2)^2 - b^2\omega^2]} \quad 3.6$$

When the generator is close to resonance,  $\omega = \omega_n$ , the power dissipation would be largest and reaches maximum [50]. The maximum dissipated power is:

$$P_{AV} = \frac{\omega_n^3mY^2}{4\zeta} \quad 3.7$$

Where  $\zeta$  is the induced damping factor can be in electrical and mechanical part in fa form It is given by  $\zeta = \zeta_m + \zeta_e$ .

In other words, The power dissipation is the sum of maximum electrical energy extracted by the transduction mechanism  $P_e$  and mechanical loss  $P_m$ .  $P_m$  and  $P_e$  are as follows:

$$P_m = \frac{\zeta_m\omega_n^3mY^2}{4\zeta} \quad 3.8$$

$$P_e = \frac{\zeta_e\omega_n^3mY^2}{4\zeta} \quad 3.9$$

In order to achieve maximal power output of device, the maximum power conversion from mechanical domain to electrical domain occurs when  $\zeta_m = \zeta_e$ , i.e. damping arising from the electrical domain equals mechanical losses. Therefore, the maximum electrical power that can be extracted by the vibration energy harvester,  $P_e$ , is given by:

$$P_e = \frac{P_{AV}}{2} = \frac{\omega_n^3mY^2}{16\zeta_m} \quad 3.10$$

Since the peak acceleration of the base  $a$  is given by  $a = Y\omega_n^2$ , equation 3.10 can be rewritten as:

$$P_e = \frac{ma^2}{16\omega_n\zeta_m} \quad 3.11$$

As the open circuit Q-factor,  $Q_{OC} = \frac{1}{2\zeta_m}$ , equation 3.11 can be written as:

$$P_e = \frac{ma^2}{8\omega_n} Q_{OC} \quad 3.12$$

### **3.2.3. Different technologies conversion in vibration energy harvesting**

As stated in the introduction, technology exists to convert ambient vibration to electricity, but the main types are electromagnetic, electrostatic and piezoelectric conversion. In the following sections, these different technologies are presented.

#### ***3.2.2.1 Electromagnetic conversion systems***

Faraday was the first to discover the electromagnetic phenomenon. Electromagnetic induction is a production of electrical current in the conductor when it is moved within a magnetic field. This is why it is characterized by a law called the Faraday Law. Several systems of vibration energy harvesting are based upon the movement of a permanent magnet inside a coil. This movement creates a current in the coil and on the surface of the coils proportional to the variation of the magnetic flux in the coil, therefore proportional to the velocity of the magnet. Figure 3.2 shows two examples of electromagnetic conversion frequently observed [51]. In electromagnetic conversion, the conductor of the electricity is done via the coil and the strong magnetic field produced by the permanent magnets. Between the coil and the permanent magnet, if one side is attached to the inertial mass then the other side is fixed to the frame. The electrical energy is generated by vibration of the relative displacement that makes the transduction mechanism. The transduction mechanism, which

generates electrical energy, is initiated by relative displacement caused by the vibration.

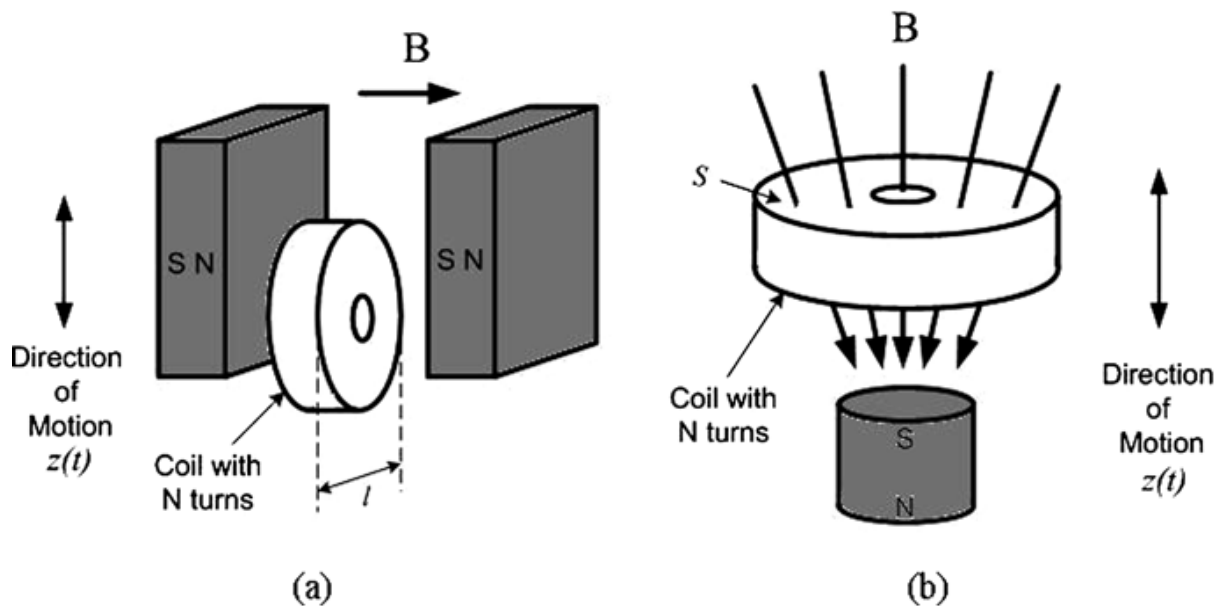


**Figure 3. 2: Electromagnetic conversion [51]**

In Figure 3.2 (a), the cutting of the magnetic field of the coil varies as a function of the relative movement among the coil and magnets. In Figure 3.2 (b), there is a distance between the magnets of the magnetic field. In the two events, the induced voltage is a function of the relative moving velocity and is determined by following equation:

$$e_m = k \times \frac{dz}{dt} \quad 3.13$$

Where:

$k$  Electromagnetic coupling factor which corresponds to  $-N \times l \times B$  for the first case (Figure 1a) and the second case (Figure 1b) to  $-N \times S \times \frac{dB}{dz}$ , both representing the variation in coupled flux per unit displacement;

$N$  The number of turns in the coil;

$l$  The effective length of the coil [m];

$B$  The flux density across the coil [T];

$\frac{dz}{dt}$  The relative velocity among the magnet and coil by time;

$S$  The effective area of the coil [ $m^2$ ];

$\frac{dB}{dz}$  The gradient of the magnetic flux density between the coil and magnet by velocity.

Figure 3.3 shows an electromagnetic generator conversion circuit together with resistance of the load  $R_L$  where the induced *e.m.f* and the current through the load are connected and given by Equation 3.14 below:

$$e.m.f + i \times (R_L + R_C) + L_C \frac{di}{dt} = 0 \quad 3.14$$

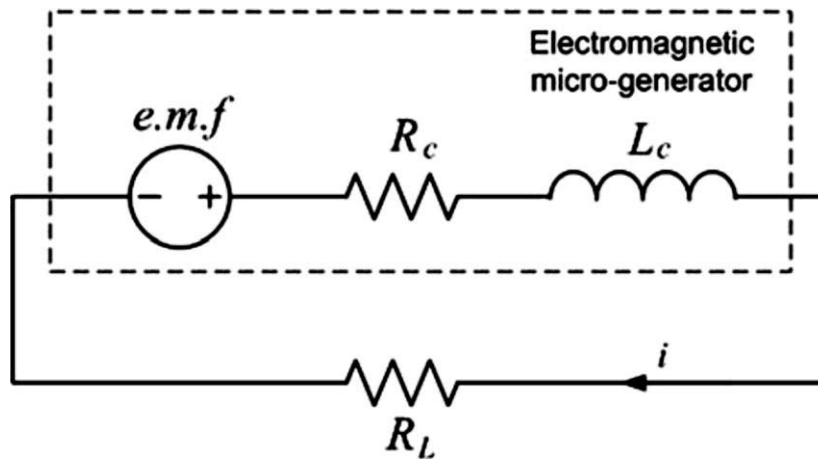


**Figure 3. 3: Circuit of electromagnetic generator conversion**

Usually the simplest structure used is a mobile magnet and fixed coils, or *vice versa*. The damping coefficient of induced electromagnetic conversion  $b_e$ , for calculating the power harvesting output, is given by:

$$b_e = \frac{k^2}{R_C + R_L + j\omega L_C} \quad 3.15$$

Where:

$R_C$  Resistance of the coil [ $\Omega$ ];

$R_L$  Resistance of the load [ $\Omega$ ];

$L_C$  Inductance of the coil [H];

$\omega$  Angular frequency of vibration [rad.s<sup>-1</sup>].

When the electromagnetic conversion operates at frequencies of low resonance, the resistive impedance is larger than the impedance of the coil. Therefore, the inductive impedance is negligible and the damping coefficient of induced electromagnetic transduction  $b_e$  becomes [50]:

$$b_e = \frac{k^2}{R_C + R_L} \quad 3.16$$

The damping factor electrically induced,  $\zeta_e$ , is given by:

$$\zeta_e = \frac{k^2}{2m\omega(R_C + R_L)} \quad 3.17$$

In Equation 3.16,  $R_L$  can vary from  $b_e$  to  $b_m$  (the parasitic damping coefficient) and thus the power output can be maximized. The load resistance optimum and the maximum power load are given by the following expressions [50]:

$$R_L = R_C + \frac{k^2}{b_m} \quad 3.18$$

$$P_e = \frac{ma^2}{16m\omega_r \left(1 - \frac{R_C}{R_L}\right)} \quad 3.19$$

Where:

$b_m$  Parasitic damping coefficient;

$a$  Acceleration of the vibration [ms<sup>-2</sup>];

$m$  Seismic mass [g];



$\omega_r$  Resonant frequency [Hz].

### 3.2.2.2 Electrostatic conversion systems

Energy harvesting by electrostatic conversion can be accomplished by two conductors isolated by a capacitor which vibrate relative to each other. By varying the distance between the conductors, the stored energy in the condenser changes thereby becoming a device converting mechanical energy into electrical energy. Unlike electromagnetic and piezoelectric conversion systems, electrostatic conversion systems need to be preloaded before producing electricity (power) and they are mechanically limited to prevent contact between the conductors causing a short circuit.

Electrostatic conversions are classified into three categories [51]:

- Figure 3.4 (a) shows electrostatic conversion *in plane overlaps varying* in which the overlap area varies between finger electrodes.
- Figure 3.4 (b) shows electrostatic conversion *in plane gap closing* where the gap varies among finger electrodes.
- Figure 3.4 (c) shows electrostatic conversion *out of plane gap closing* where the gap varies between the two main electrode plates [51].

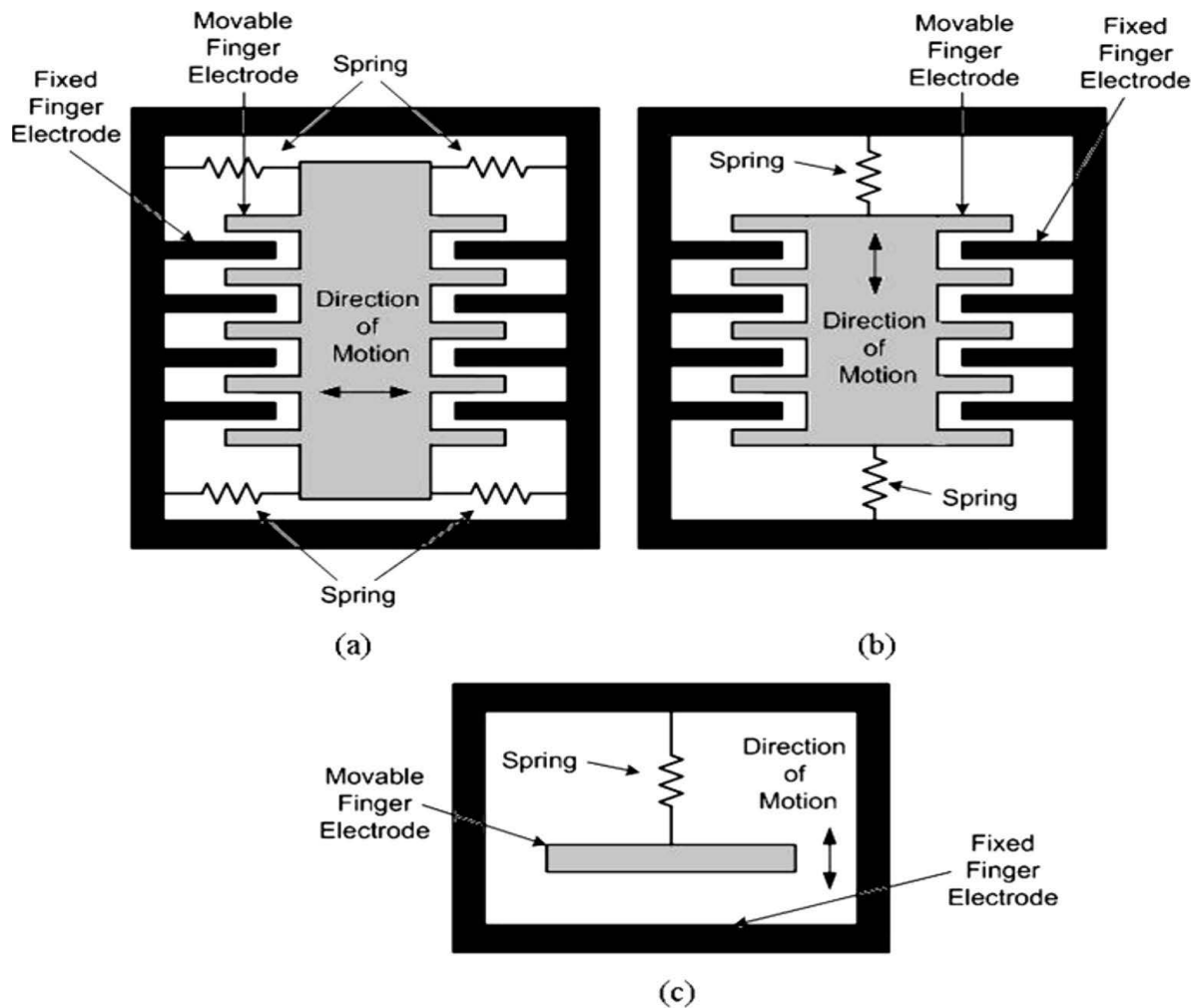


**Figure 3. 4: Electrostatic conversion [51]**

These three categories can be used in constant voltage cycles or in constant charge cycles.

➤ *For the constant voltage cycles:*

The constant voltage cycles also starts when the capacitance of the electrostatic converter is maximal. The capacitor is polarized at a voltage  $E_{V.cst}$  using an external supply source such as battery, charged capacitor, etc. This voltage will be maintained throughout the conversion cycle thanks to an electronic circuit. Since the voltage is constant and the capacitance decreases, the charge of the capacitor increases, generating a current that is scavenged and stored. When the capacitance reaches its minimum value, the charge  $Q$  still presents in the capacitor is completely collected and stored. The total amount of energy converted at each cycle is presented in equation 3.20 [52].

$$E_{V.cst} = \frac{1}{2} V^2 (C_{min} - C_{max}) \quad 3.20$$

Where:

$V$  Voltage to the terminals of the structure [V];

$C_{max}$  Maximum coupled [Nm];

$C_{min}$  Minimum coupled [Nm].

➤ *For the constant charge cycles:*

The constant charge cycle is the easiest one to implement on electrostatic devices. The cycle starts when the structure reaches its maximum capacitance  $C_{max}$ . In this position, the structure is charged thanks to an external polarization source: an electric charge  $E_{Q.cst}$  is stored in the capacitor under a given voltage  $V_{min}$ . The device is then let in open circuit. The structure moves mechanically to a position where its capacitance is minimal. As the charge  $Q_{cst}$  is kept constant while the capacitance  $C$  decreases, the voltage across the capacitor  $V$  increases. When the capacitance reaches its minimum ( $C_{min}$ ) (or the voltage its maximum ( $V_{max}$ ), electric charges are removed from the structure. The total amount of energy converted at each cycle is presented in equation 3.21 [52].

$$E_{Q.cst} = \frac{1}{2} Q^2 \left( \frac{1}{C_{min}} - \frac{1}{C_{max}} \right) \quad 3.21$$

Where:

$Q$  Electric charge [V];

$C_{max}$  Maximum coupled [Nm];

$C_{min}$  Minimum coupled [Nm].

In general, the generators supply more energy in constant voltage cycles electrostatic conversion than in constant charge cycles electrostatic conversion. The mechanical motion imposed on the structure where the energy is stored, allows for varying of the value of this capacity. Due to the constant charge ( $Q = CV$ ), when the plates move away, the voltage

across it increases. Finally, the loads are removed from the structure in its minimum capacity. The electrical energy harvested is greater than the energy initially injected. Electrical energy is amplified by the mechanical energy [52].

Figure 3.5 represents a circuit using charge constrained electrostatic conversion.

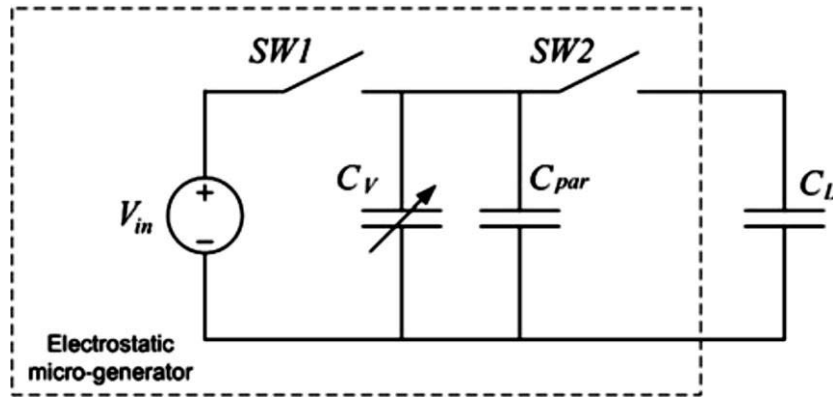


**Figure 3. 5: Circuit of electrostatic conversion charge constrained**

In the above circuit,  $C_L$  is the storage capacity,  $C_{par}$  is the parasitic ability coupled with any interconnection structure and the variable capacitor, and this limits the maximum voltage.  $C_V$  represents a variable capacitor and  $V_{in}$  is a pre-charged tank, which may be a rechargeable battery or a capacitor.

The maximum voltage at the terminals of the load,  $V_{max}$ , is given by the following expression:

$$V_{max} = \frac{C_{max} + C_{par}}{C_{min} + C_{par}} V_{in} \quad 3.22$$

As the energy is dissipated in the damper, the force distance product gives the power and the equation of the power  $P$  is:

$$P = \frac{4YF\omega\omega_c^2}{2\pi} \sqrt{\frac{1}{1 - \omega_c^2} - \left(\frac{F}{mY\omega^2\omega_c}\right)^2} U \quad 3.23$$

Where:

$F$  Damping force [N];

$Y$  Displacement of the frame [m];

$\omega$  Angular frequency of vibration [rad.s<sup>-1</sup>];

$m$  Seismic mass [kg];

$\omega_c$  Angular frequency of cantilever [rad.s<sup>-1</sup>] and it's given by  $\omega_c = \frac{\omega}{\omega_r}$ .

The optimum damping force is:

$$F_{opt} = \frac{Y\omega^2 m}{\sqrt{2}} \frac{\omega_c}{|(1 + \omega_c^2)U|} \quad 3.24$$

Where  $U$  is the ratio of angular frequency of cantilever beam and is equal to  $U = \frac{\sin(\frac{\pi}{\omega_c})}{1 + \cos\frac{\pi}{\omega_c}}$ .

Table 3.2 gives the variation of the electrostatic force for all three setups.  $x$  represent the displacement of the inertial mass [53].

**Table 3.2: Electrostatic force variations [53]**

Structure	Voltage constrained	Charge constrained
<i>In plane overlaps varying</i>	$F_e$ constant	$F_e=1/x^2$
<i>In plane gap closing</i>	$F_e=1/x^2$	$F_e=1/x$
<i>Out of plane gap closing</i>	$F_e=1/x$	$F_e$ constant

### 3.2.2.3 Piezoelectric conversion system

The word "piezoelectric" means electricity caused by pressure. The first researchers to have studied this phenomenon were Pierre and Jacques Curie in 1880. They found out an unusual feature of some crystal materials, whereby the crystals became electrically polarized when subject to mechanical action. In tension and compression force, they are producers of

voltages of opposite polarity proportional to the force applied which can be in mode 33 or mode 31, Figure 3.6 shows the behaviours of the piezoelectric effect. In addition, if a voltage generating crystal is subjected to an electric charge, it shortens or grows in proportion to the intensity of the charge depending on the polarity of the field [12].

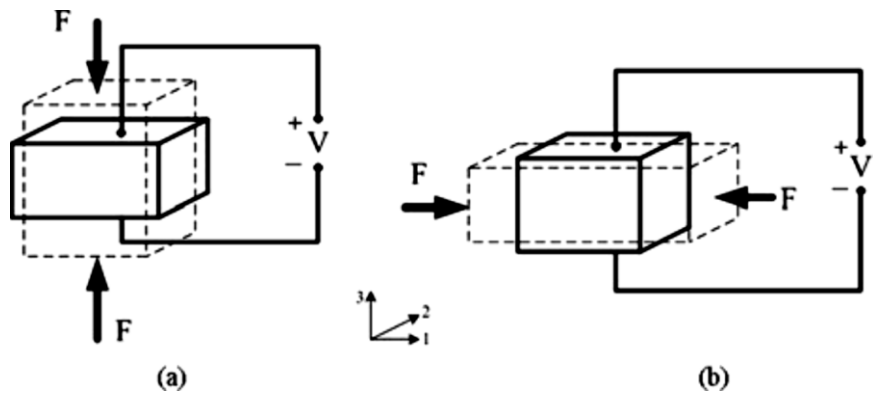


**Figure 3. 6: Piezoelectric conversion: (a) mode 33 and (b) mode 31 [51]**

Piezoelectric conversion is able to produce high electrical energy unlike electromagnetic conversion because piezoelectric conversion provides useful voltages and exhibits higher practical energy densities. It does not need an external power supply, unlike electrostatic conversion. It is for these reasons that the option of piezoelectric conversion is chosen in this study.

Figure 3.7 represents a circuit in series representing a piezoelectric conversion generator, with resistive load  $R_L$ , capacitance  $C$  between two electrodes and resistance  $R_S$ .

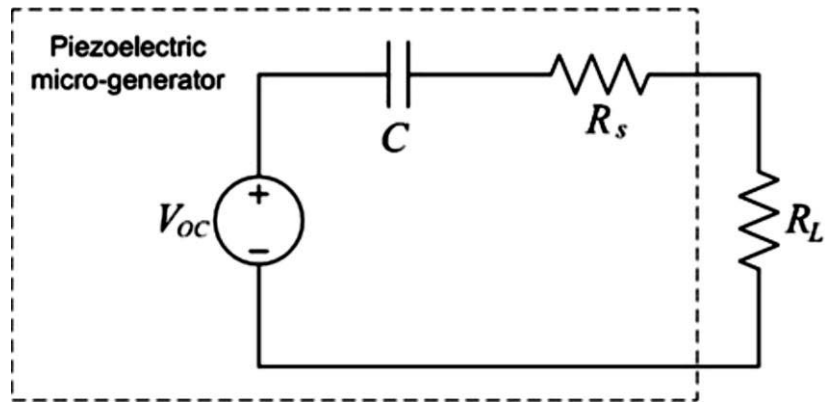


**Figure 3. 7: Generator circuit piezoelectric conversions**

The voltage supply is the open circuit voltage when the electrical displacement resultant is equal to zero.

$$V_{OC} = -\frac{d \times t}{\varepsilon} \times \sigma \quad 3.25$$

Where:

- $d$  Piezoelectric strain coefficient [-];
- $t$  Thickness of piezoelectric material [m];
- $\varepsilon$  Dielectric constant of piezoelectric material [-];
- $\sigma$  Mechanical stress [ $\text{Nm}^2$ ].

Therefore, the piezoelectric damping coefficient is an important property and it is not given by manufacturer. The piezoelectric damping coefficient is related to mechanical loss and it is dependent of the frequency. It is important to know a precise piezoelectric damping coefficient value and other properties to model piezoelectric material, because piezoelectric material design involves mathematical modeling and experimental verification, which are necessary to validate the piezoelectric materials.

The expression of the piezoelectric damping coefficient is as follows:

$$b_e = \frac{2m\omega^2 k^2}{2\sqrt{\omega_r^2 + \frac{1}{R_L C_L}}} \times \sigma \quad 3.26$$

Where:

$k$  Electromechanical coupling factor of piezoelectric material;

$C_L$  Load capacitance.

$R_L$  Load resistance.

At the maximum power generation, there is an optimal load. By optimizing  $R_L$  to the conversion system, the optimum value is given by equation 3.27 [24].

$$R_{opt} = \frac{1}{\omega_r C} \times \frac{2\zeta_m}{\sqrt{4\zeta_m^2 + k^4}} \quad 3.27$$

Where:

$C$  Capacitance between two electrodes [F];

$\zeta_m$  Damping factor mechanically induced;

$k$  Electromechanical coupling factor of piezoelectric material.

The maximum power  $P_{max}$  occurs when  $\zeta_e = \zeta_m$  and is given by [24]:

$$P_{max} = \frac{1}{\omega_r^2} \times \frac{R_L C^2 \left(\frac{2Ydtb^*}{\epsilon}\right)^2}{(4\zeta_m^2 + K^4)(R_L C \omega_r)^2 + 4\zeta_m K^2 (R_L C \omega_r) + 2\zeta_m^2} a^2 \quad 3.28$$

Where:



$b^*$	Constant linked to the size of the piezoelectric generator;
$a$	Acceleration of the vibration [ $\text{ms}^{-2}$ ];
$\omega_r$	Resonant frequency [Hz];
$\zeta_m$	Damping factor mechanically induced;
$d$	The piezoelectric strain coefficient;
$t$	Thickness of the piezoelectric material [m];
$\varepsilon$	Dielectric displacement per unit electric field and compliance;
$k$	Electromechanical coupling coefficient;
$Y$	The displacement of the frame [m];
$R_L$	Resistance of the load [ $\Omega$ ].

### 3.2.3 Summary of different types of conversion technologies

Roundy [28] has provided a general theory which may be used to relate numerous designs and approaches according to vibration energy harvesting generators. The theory can be applied to the different technologies conversion of vibration energy harvesting. Each of them, including piezoelectric conversion systems, has received considerable attention because they do not need an external power source due to their high electromechanical coupling. In particular, the piezoelectric conversion system is attractive for use in MEMS [48], [54], [55].

Table 3.3 gives a summary of advantages and disadvantages of different conversion technologies.

**Table 3.3: Summary of different conversion technologies [24].**

<b>Types of conversion</b>	<b>Development level</b>	<b>Miniaturization</b>	<b>Power output density</b>	<b>Specific problems</b>
<b>Electromagnetic</b>	Advanced macroscale, limited at the microscale.	- Difficult at the integration of materials.	- High on the macroscale. - Decreases with volume.	- Low output voltage. - Difficult integration.
<b>Electrostatic</b>	Advanced macroscale and microscale.	- Easy integration of materials. - Problem of the realization of the structure.	- Low on the macroscale. - Increases with decreasing volume.	- Need for polarization source. - High voltage. - Mechanical guidance.
<b>Piezoelectric</b>	Average in the macroscale and microscale.	- Slightly lower performance of materials in thin layers.	- High on the macroscale. - Decreases at the microscopic level due to the properties of materials.	- Materials in thin layers a little less efficient than solid materials. - Limited performance due to the coupling coefficient of the materials.

In the literature review and Chapter Three, we illustrated an overview of the energy requirements of a variety of electronic system devices. We have detailed the various conversions available to recover or to harvest energy from environmental vibration paying special attention to levels of output power obtained in experiments to date. In our study we have chosen Piezoelectric conversion for all our experiments and theory.

## CHAPTER FOUR

# PIEZOELECTRIC ENERGY HARVESTING FROM VIBRATION

---

### 4.1 Overview of Piezoelectricity

The word piezoelectricity, from Greek “piézein” or “piezo” meaning “to press” or “to squeeze” and “electric” or “electron”, means electricity resulting from user pressure. By definition, piezoelectricity is the electrical load that builds up in certain solid materials under the action of mechanical stress or in response to applied mechanical stress. Conversely or inversely, these materials can be deformed under the action of an electrical field [56]. This thesis is based on piezoelectricity where the mechanism is to transfer energy from mechanical vibration into electrical energy. It follows that a description of the concept is warranted, so that an understanding of the background and fundamentals of this phenomenon may be gained.

### 4.2 Brief History of piezoelectricity

The idea that some solid materials might exhibit an electrical response when subjected to pressure was initially shown conclusively by the French sibling physicists Pierre and Jacques Curie in 1880. Based on their knowledge of the crystallographic origins of pyro electricity (the ability of a solid to develop an electrical charge in response to a change in temperature), they put forward the theory that there was a one to one interdependence between the electrical effects resulting from a variation of temperature and the mechanical strain in the crystal. The Curie brothers called this the “piezoelectric effect” (direct piezoelectric effect). They proved the effect by using solid materials like quartz, cane sugar, crystals of tourmaline, Rochelle salt, and topaz.

The Curie brothers announced their discovery as follows:

*“Those crystals having one or more axes whose ends are unlike, that is to say, hemihedral crystals with oblique faces have the special physical property of giving rise to two electrical poles of opposite signs at the extremities of these axes when they are subjected to a change in temperature: this is the phenomenon known under the name of pyroelectricity. We have found a new method for the development of polar electricity in these same crystals, consisting in subjecting them to variations in pressure along their hemihedral axes” [57].*

The Curie brothers did not discover the converse piezoelectric effect. The piezoelectric converse effect, by definition, is when an imposed voltage produces mechanical deformations or strains on the material, or wherein a constraint is described in the material when an electric charge is implemented. The first scientist to describe the converse piezoelectric effect was Gabriel Lippman in 1881. He deduced this mathematically from fundamental thermodynamic principles. The Curie brothers agreed with this finding, finding quantitative evidence of the full reversibility of the electro-elasto-mechanical deformation. The name “piezoelectricity” was suggested by Wilhelm Gottlieb Hankel which became the accepted name for the effect[58].

The Curie brothers continued to study the properties of this new phenomenon using only one type of crystal (tourmaline). The direction they took was to perform systematic quantitative experiments in order to discover the rules governing the effect [57]. Such rules had already been found for pyroelectricity, and given the analogous links the two phenomena shared the reasoning was that similar laws existed for piezoelectricity. In January 1881 to the Academy of Science, following from their experiments, confirmed their new found rules [57]:

- The two ends of a tourmaline crystal release quantities of electricity which are equal and of opposite sign.
- The quantity released by a certain increase in pressure is of opposite sign and equal in magnitude to that produced by an equal reduction in force.
- The quantity is proportional to the variation in force.
- It is independent of the length of the tourmaline crystal.

- For the same variation of force per unit area it is proportional to that area.

The core of applied piezoelectric science was established within only two years of publication of the above rules, through collaborative work in the European scientific community. This core was: the usefulness of thermodynamics to quantify the complex relationships between electrical, thermal and mechanical variables; identification of piezoelectric crystals based on the unequal crystal structure, and; the alterable interchange of both mechanical and electrical energy.

Within a few decades, a lot of work had been done to explore both the crystal structures fully defining 20 natural classes of crystal that exhibited piezoelectric effects and the 18 most important macroscopic piezoelectric coefficients accompanying the thermodynamic processing of crystal solids using tensional analysis. The standard reference work at that time, by Woldemar Voigt, was published in 1910 (*Lerbuch der Kristallphysik: Textbook on Crystal Physics*).

The initial major application of piezoelectricity were in the development of sonar during the First World War in 1917. The French physicist Paul Langevin and his colleagues began to solve the problem of ultrasonic submarine detection [58]. They used a transducer which was a mosaic crystals thin quartz bonded between two steel sheets mounted in a housing suitable for immersion. The resonant frequency of device was about 50 KHz and emitted a high frequency chirp undersea and measured depth by measuring the time of the return echo. Since then the development of materials, circuits, sonar transducers and systems has been ongoing [59].

The success of sonar, both, led scientists to increase development activity for all types of piezoelectric devices resonating and non-resonating. Possibly the next major technological milestone in the advancement of piezoelectricity was the development of the 'crystal oscillator'. A crystal exhibiting the piezoelectric effect can be made to resonate by driving it at its natural mechanical frequency. Because the frequency dependence on temperature is very low, such piezoelectric resonators can be used in applications that require very stable and accurate timing. In 1917 Alexander M. Nicholson was the first to patent a crystal oscillator developed using Rochelle salt and Walter Guyton Cady promoted the first oscillator

based on Quartz crystal in 1921. Soon after that, around 1926, for the first time, a quartz oscillator was used to stabilize the frequency of a transmitter [60]. Today, such devices are frequently used in everyday electronic systems such as wristwatches, radios, mobile phones and computers, as well as in test and measurement equipment such as oscilloscopes and signal generators.

During the Second World War, in Japan, Soviet Union (Russia) and United States, isolated scientific research groups working on the development of materials capacitor simultaneously discovered that some ceramic materials exposed to high dielectric constants up to 100 times higher than conventional crystals. The discovery of improved piezoelectric properties using ceramics prepared by sintering with metallic oxide powders ferroelectric led to intense development and research in piezoelectric devices. A significant milestone was the development of the first manufactured piezoelectric substance: barium titanate ( $\text{BaTiO}_3$ ), which led to the development of the piezoceramics lead zirconate titanate family in 1950 [59]. A large number of products and applications for piezoelectricity emerged out of the research efforts during World War II, including: improved sonar devices, piezoelectric filters, piezo buzzers, phonograph ‘pickups’ for record players, igniters (similar to those used in gas grills), and microphones.

In the 1960s discoveries were made concerning the piezoelectric properties of some polymer materials. In 1969, Kawai et al. discovered that polyvinylidene had some piezoelectric properties after being stretched during fabrication [61].

Over time, the market for piezoelectric products has increased leading to the development of many significant products utilising Surface Acoustic Wave effects to attain high frequency signal filtering (SAW filter devices), air ultrasonic transducers (intrusion alarms and television remote controls) and audio buzzers (TTL compatible tone generators and smoke alarms) [60].

### **4.3 Piezoelectric effect**

Piezoelectricity is the charge separation within a material sensitive to an applied strain. It is also the property of certain materials to electrically polarize when deformed [56]. This effect

is achieved in crystals that do not have any centre of symmetry. One needs to look at the molecules which make up the crystal to explain this effect. Each of the molecules has a polarization. If one end is positively charged the other end is negatively charged and is called a dipole. This is the result of the atoms which constitute the molecule and how they are materialized. Figure 4.1 illustrates this process. The polar axis is an imaginary line passing through the centre of the two charges on the molecule. In the mono crystal shown in Figure 4.1 - (a), the polar axes of the dipoles are all located in one direction. The crystal is said to be symmetric because if you cut the crystal at any point, the polar axes of the two resulting pieces are in the same direction as the original. In the poly crystal shown in Figure 4.1 - (b), within the material, there is a different polar axis for different regions. It is asymmetric because there will not be the same polar axis if the crystal is cut into two pieces.

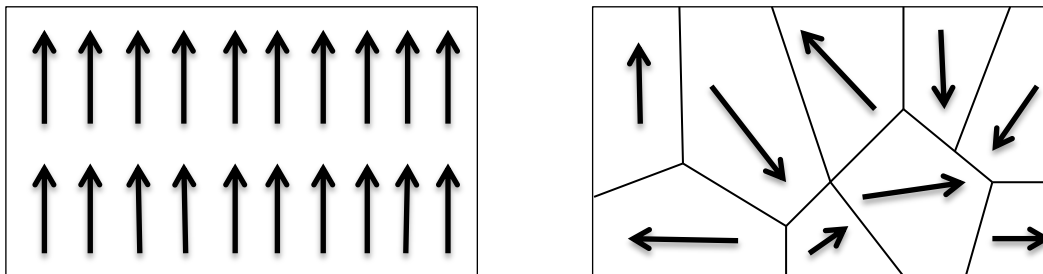


**Figure 4. 1: (a) Mono crystal with single polar axis. (b) Poly crystal with random polar axis.**

To produce the piezoelectric effect, the poly-crystal, Figure 4.1 (b), is warmed under application of a large electric field. The warmth lets the molecules move about more freely and the electric field strength in the crystal alignment for all the dipoles is approximately in the same direction.

For macroscopic piezoelectricity to be observed in the material (where charge separation can be observed across the whole of the material and used to perform work) a ‘poling’ process first has to be completed. The poling treatment involves exposing the material to a strong electric field at an elevated temperature; usually a temperature just below the Curie temperature of the material (the Curie temperature is the critical point where a material's intrinsic magnetic moment change direction). Under these conditions, the electrical dipoles most nearly aligned with the direction of the applied field will grow and the dipoles that are not initially aligned will orientate themselves to become more in-line. On removal of the

electric field and elevated temperature conditions, the dipoles remain locked in approximate alignment, thus giving the material remnant polarization and making it piezoelectrically active. Figure 4.2 illustrates this process.

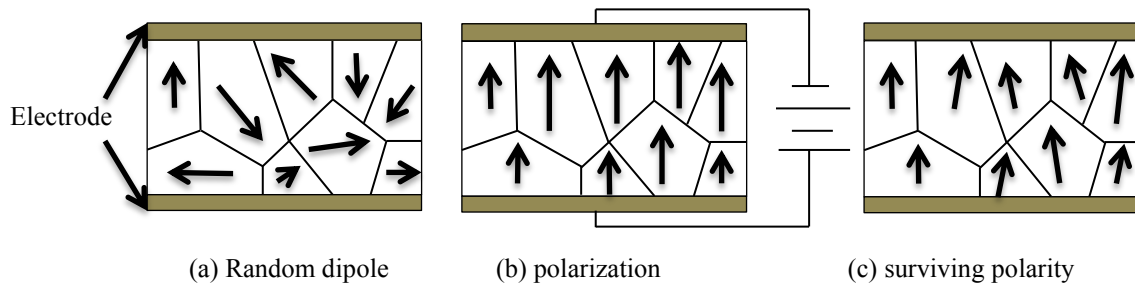


**Figure 4. 2: Polarization of ceramic material to generate piezoelectric effect.**

In general, piezoelectricity is manifested by two effects, namely, the direct and converse piezoelectric effect. In the piezoelectric effect, the materials have the ability to convert mechanical strain into electrical charge while the converse piezoelectric effect, the materials have the ability to convert an applied electrical potential charge into mechanical strain energy. These two domains are illustrated in Figure 4.3.

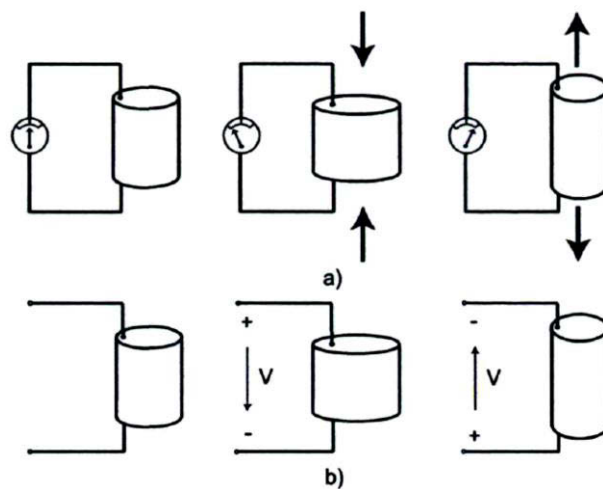


**Figure 4. 3: (a) Direct piezoelectric effect and (b) Converse piezoelectric effect.**

### 4.3.1 Direct piezoelectric effect

In this first approach, the conversion of mechanical energy to electrical energy is direct, that is to say, without any intermediate storage of energy in mechanical form (the intermediate



storage in question could be, for example, a mass moving or vibrating structure). It sets the rate of electromechanical conversion as the ratio of electrical energy recovered to the mechanical energy supplied. This size does not correspond precisely to performance, because the piezoelectric material renders energy when the constraint is removed. However, considering that the restored energy is lost or unusable, which is usually the case for micro-generators direct conversion, then the conversion rate can be equated with the conversion efficiency.

#### 4.3.2 Converse piezoelectric effect

Rather than excite a piezoelectric materials on its own, an easier way is to paste piezoelectric materials onto a vibrating structure such as a beam. If one end of the beam is encased in a stationary frame, and the other end is left free, when the structure is excited by an outside force the converted energy is dissipated in a resistor load. The performance of this device is the ratio of the energy generated in the load to the power supplied to the beam.

The direct and converse piezoelectric effects can be expressed mathematically by two linearized equations. These mathematical models have four variables (two mechanical and two electrical variables) and can be converted by a set of nine equations and are called the piezoelectric constitutive law. The IEEE standard on piezoelectricity gives various series of constants used in conjunction with the axes notation [62]. According to this standard, the Electric displacement  $D$  and Strain  $S$  are given by Equations 4.1 and 4.2.

$$D = d\sigma + \varepsilon^{\sigma} E \quad 4.1$$

$$S = s^E \sigma + dE \quad 4.2$$

Where:

$D$  Polarization [ $C/m^2$ ];

$d$  Piezoelectric charge coefficient [ $m/V$  or  $C/N$ ];

$S$	Strain [m/m];
$\sigma$	Stress [N/m <sup>2</sup> ];
$E$	Electric field [N/C or V/m];
$\epsilon^\sigma$	Dielectric constant (permittivity) under constant stress [F/m];
$s^E$	Compliance when the electric field is constant [m <sup>2</sup> /N] (the superscript $E$ denotes that the electric field is constant).

#### 4.4 Piezoelectric materials

This section considers the modes of piezoelectric materials and outlines different types of piezoelectric materials and their properties.

##### 4.4.1. Modes of piezoelectric materials

The recovery of energy using piezoelectric materials enables for a device that is self-catering, that is to say which does not need any external supporting attributes. Applying a constraint on a piezoelectric material causes the occurrence of a voltage between the electrodes. Moreover, the piezoelectric materials are capable of producing power at voltage levels which can be easily conditioned. Piezoelectric material can be configured so that the mechanical stress is perpendicular or parallel to the electrodes. As a result of compression and tension force, the opposite polarity voltages proportionate to the applied force can be produced, which can be in mode 33 or mode 31 as shown in Figure 3.5 [51].

##### 4.4.2. Different types of piezoelectric materials

There are many kinds of piezoelectric materials that can be used to harvest ambient vibration energy but the main classes are: piezoelectric materials ceramics, crystals that have a natural piezoelectricity, macro fiber composite (MFC), polymers and polarized composites.

###### *A. Ceramics*

The first piezoelectric materials based on synthetic Barium Titanate appeared after 1945. Lead Zirconate Titanate materials (PZT) developed from 1945 spread very quickly because

their characteristics far superseded those of all other piezoelectric materials. They are used in active control structures as actuators and sensors and can be included in the composition of active composite materials

### *B. Crystals (Crystallines)*

The most well-known of piezoelectric crystals is quartz but its performance in terms of properties is unattractive for applications in vibration. Other materials, such as lithium niobate ( $\text{LiNbO}_3$ ) and lithium tantalite ( $\text{LiTaO}_3$ ) show higher values of coupling coefficient but the high cost and fragility of these crystals explains why they are uncommon in current products

### *C. Polymers*

Some polymers such as PVDF (polyvinylidene fluoride) and copolymers such as PVDF-TrFE can acquire piezoelectric properties. They possess a thickness which may be very low and a high flexibility which makes them suitable for non-planar surfaces. They have been tested and are used in various applications. They are effective as sensors, thanks to their low hysteresis. However, their low electromechanical coupling coefficient penalises them as actuators. They have high dielectric losses.

### *D. Composites*

These are bulk ceramics. These materials, first developed for sonar applications, were introduced in the early 1980s and represented a major breakthrough in the field of piezoelectric materials, since the appearance of PZT in the 1960s.

The most commonly used are ceramics of lead zirconate titanate (PZT) and polyvinylidene fluoride (PVDF) [48]. Table 4.1 shows the properties of these materials. In general, the piezoelectric material is coupled to a resonant structure which imposes a strain or vibration. Due to piezoelectricity, this deformation is converted into electrical charge by different means which are compressed, slap and bending.

**Table 4.1: Some properties of common piezoelectric materials [5]**

<b>Material</b>	<b>BaTiO<sub>3</sub></b>	<b>PZT 5A</b>	<b>PZT 5H</b>	<b>PVDF</b>
$d_{31} (\times 10^{-12} \text{ CN}^{-1})$	78	-171	-274	23
$d_{33} (\times 10^{-12} \text{ CN}^{-1})$	149	374	593	-33
$g_{31} (\times 10^{-3} \text{ VmN}^{-1})$	5	-11.4	-9.1	216
$g_{33} (\times 10^{-3} \text{ VmN}^{-1})$	14.1	24.8	19.7	330
$k_{31}$	0.21	0.31	0.39	0.12
$k_{33}$	0.48	0.71	0.75	0.15
<b>Relative permittivity (<math>\epsilon/\epsilon_0</math>)</b>	1700	1700	3400	12
<b>Young's modulus (GPa)</b>	67	50	50	2

#### 4.4.3. Advantages of piezoelectric materials

Currently, metal based piezoelectric ceramic oxides and other synthetic materials allow designers to use the direct and the converse piezoelectric effect in several new applications. These materials are generally chemically inert and stronger physically. They also have a large electromechanical couple constant and provide a high energy conversion rate. Their compactness, bandwidth and performance are ever expanding elements of choice for vibration control of flexible structures. Concerning manufacture, they are relatively inexpensive. There are several types with different advantages. For example, piezoceramics offer great structural rigidity which gives them a large active power, while the flexibility of piezoelectric film gives them a high sensitivity. The size and shape of a piezoceramic device can be adapted to respond to a specific goal because of their fragility (e.g., plates, discs, cylinders, rings). These materials can interact with frequencies from several Hertz to megahertz making them useful for a wide range of applications. The operating temperatures of ceramics based on formulations of lead zirconate titanate are higher compared to other ceramic compositions and the materials "PZT" are presently the most widely used [63].

Moreover, given the relatively low weight of piezoelectric materials, a large amount of these devices can be used without significantly increasing the weight of the structure.

## CHAPTER FIVE

### EXPERIMENTAL SETUP AND METHODOLOGY

---

#### 5.1 Background

The main aim of this work was to gather ambient energy from vibration sources in the form of mechanical energy and convert it into electrical energy using piezoelectric materials. Based upon consideration raised before, the objective target for this experiment was to measure the voltage output (electrical energy) generated by the prototype generator for the two setups and compare them. In this experiment, in order to convert the vibration mechanical energy into electrical energy, two types of setup of prototype generators were used. The first setup consists of a cantilever beam without a concentrated tip mass. The second setup consists of a concentrated tip mass at one end of a cantilever beam. In the following chapter, the details on its are explained. Both operated at the same constant velocity, but produced different voltage outputs. The setup evaluates energy harnessed for high frequency vibration via a medium size energy harvester to get a high output voltage.

To achieve the experiment objective, the experiments were carried out at the Vibration Research and Testing Centre (VRTC) at the University of KwaZulu-Natal, Westville Campus, Durban, South Africa. The VRTC provides an indoor laboratory related to mechanical vibration set up according to IEC (International Electrotechnical Commission) and IEEE (Institute of Electrical and Electronics Engineers) standards. The essential components of the vibration test facility used for this research are shown in Figure 5.1.

In this chapter, some of the equipment and the material used, laboratory set up, experimental procedures and methodology for this study are presented.

#### 5.2 Experimental apparatus

The essential components of the vibration test facility used for this research are shown in Figure 5.1.



**Figure 5. 1: View of all equipment used**

In Figure 5.1, the different components visible are:

1. Computer for data acquisition system.
2. Controller.
3. Amplifier Tira.
4. Prototype generator with PZT-4 and Accelerometer.
5. Electrodynamic vibration exciter (shaker).

### **5.2.1. Equipment used**

The production of vibration in the laboratory for this study was achieved by an electrodynamic shaker, namely, TIRA Model, Type TV 56263/LS-340. Figure 5.2 shows the electrodynamic vibration exciter (shaker).



**Figure 5. 2: Electrodynamic vibration exciter shaker**

The electrodynamic shaker reproduces vibration in the ambient environment under laboratory conditions for testing the dynamic strength and the reliability in all fields of applications of vibration testing. It is pivoted to enable the excitation in a vertical direction. In order to guarantee the performance of the system, a digital amplifier is used. In principal the electrodynamic shaker operates like a speaker where the armature movement is created by an electrical current in the coil. The coil produces a magnetic field which is opposite to the static magnetic field produced by the electromagnet in the shaker. Electrical power (voltage and current) is provided to the armature of the shaker through the amplifier shown in the Figure 5.3. It also provides the necessary field power supply for the cooling fan, and auxiliary supplies.





**Figure 5. 3: Amplifier Tira**

In addition to those functions, the role of the amplifier is to monitor the system interlock signals. It shuts down when any abnormality is observed in the vibration system which is a closed loop system. The controller's role is to ensure that what has been programmed is the same as the output signal from the shaker base piezoelectric material and accelerometer. The signal produced by the accelerometer and piezoelectric material pass through typical steps which include amplification, attenuation, filtration, differentiation and integration. The accelerometer is a link between the vibrating object and the measurement equipment. An accelerometer is a device which senses the motion of a component or object to which it is attached and produces an electrical voltage or current signal which is proportional to the component or object motion. The object motion is characterized by some quantity of vibration which could be acceleration, velocity, or displacement.

In this study, the piezoelectric accelerometer used was a model Bruel & Kjaer type 4507 B shown in Figure 5.4.

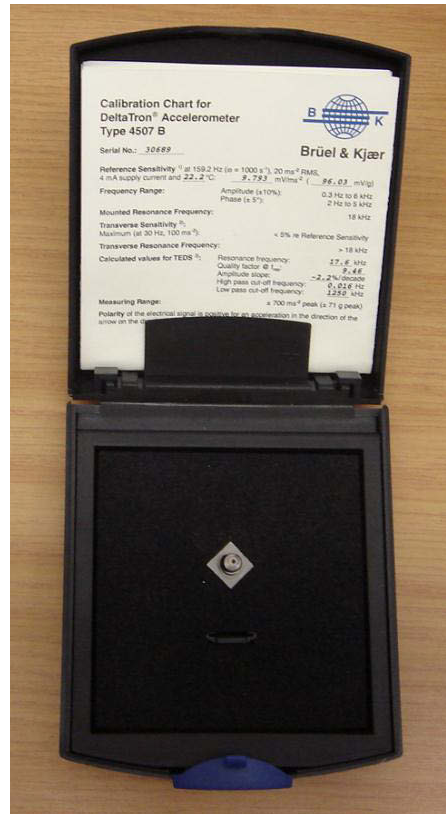


**Figure 5. 4: Piezoelectric accelerometer model Bruel & Kjaer type 4507 B**

Compared to other types of sensors, piezoelectric accelerometers are widely used in vibration research because of their advantages. Some of the important advantages of piezoelectric accelerometers are:

- Wide frequency range of measurement;
- No moving parts, therefore no wear or inertial problems;
- The accelerometer signal can be easily integrated to obtain velocity as well as displacement;
- High sensitivity.

All measurements and data were captured and given on the computer where is connected to the controller by PUMA Vibration Control and Analysis System software. Figure 5.5 shows the computer for data acquisition system and control system of PUMA Vibration Control and Analysis System software.



**Figure 5. 5: PUMA Vibration Control and Analysis System software**

#### **5.2.2. Piezoelectric material PZT- 4**

To convert vibrational energy into electrical energy from the experiment, the piezoelectric material selected and purchased was piezo-ceramic PZT (Lead Zirconate Titanate), because of its popularity, good performance characteristics and high piezoelectric coefficient. The piezoelectric materials were manufactured by Steminc: Steiner & Martins, INC., as shown in Figure 5.6. These devices are more efficient in energy conversion in comparison to other piezoelectric devices available. The length-width-thickness is  $45 \times 45 \times 2.8$  mm.



**Figure 5. 6: Picture of the piezoelectric ceramic materials PZT-4.**

This Piezoelectric Ceramic Plate is made up of different components and the different characteristics and performance are summarized in Table 5.1. It is ideal for pressure sensor and electricity generation. The silver electrode piezoelectric wafers are located one on each side (S configuration) of the piezoelectric material. The Piezoelectric Ceramic plates have a red DOT marking one of the sides which indicates the positive side and other side is the negative. For soldering wire leads, the soldering technique suggested use the soldering temperature of 250 °C - 270 °C within 3 seconds and 1 - 2 % Silver content solder material. Without these conditions, the piezoelectric materials may lose its piezoelectric properties in the final result [64].

**Table 5. 1: Different components of material for PZT-4**

<b>Components</b>	<b>Material %</b>
Lead Oxide	55-75
Zirconium Oxide	18-30
Titanium Oxide	7-20
Lanthanum Oxide	2-5

The various characteristics for this PZT-4 are:

- Dimensions: 45 x 45 x 2.8 mm
- Resonance frequency  $f_r$ : 41 Hz to  $\pm 2$  KHz
- Electromechanical coupling coefficient  $K_{31}$ :  $\geq 57$  %
- Resonant impedance  $Z_m$ :  $\leq 3 \Omega$
- Static capacitance  $C_s$ : 9000 pF  $\pm 15$  % @ 1 kHz
- Test Condition: 23  $\pm$  3 °C 40 ~70 % R.H.
- $f_r$ ,  $Z_m$ ,  $K_p$  => Lengthwise mode vibration application.
- $C_s$  => LCR meter at 1KHz 1Vrms

Electrodes can be used to recover electrical voltage along the surface of a deformed or stressed material. Thus, the piezoelectric properties should contain a sign convention for the ability to harvest electrical energy in three directions. Based on this argument, the

piezoelectric material configuration may be widespread for two cases: the stack and the bender configurations; the former operates in the 33 mode while the latter operates in the 31 mode [12, 51]. Assumptions are made that the polarization direction is constantly in the "3" direction; which gives a better understanding of the two modes of operation.

### 5.2.3. Prototype generator

The prototype generator for this study was fabricated by putting a PZT-4 shim to the top plane of a steel centre beam by means of Loctite (Henkel, Düsseldorf, Germany) superglue. Figure 5.7 shows a cantilever piezoelectric generator developed for this study.

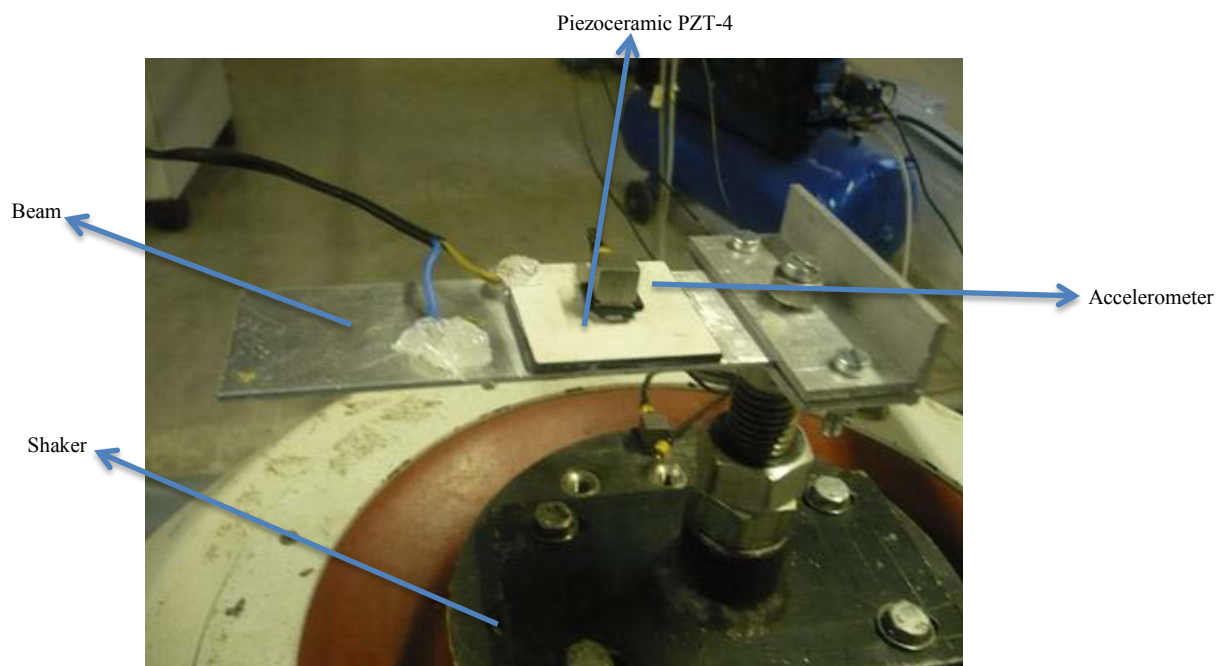


**Figure 5. 7: Picture of piezoelectric cantilever beam on the shaker**

Electrical modelling can be carried out on a piezoelectric material which has been mechanically stressed at a low frequency and this is done by a time dependent charge source, which is gathered in a capacitor. This conversion mechanism can generate electricity from the relative movement of the mechanical stress occurring in the system and the effects of deformation of the strain of the active materials used in the mechanical system. Whether it is position or velocity, the relative movement may be coupled to a transduction mechanism. The

prototype generator is fixed to the electrodynamic shaker so that the prototype generator vibrates in sync with the electrodynamic shaker. Electricity is generated once the source begins to vibrate which in turn converts vibration energy into electrical energy which produces an AC voltage. If the piezoelectric material undergoes a periodic or sinusoidal stress due to external vibrations, an AC open circuit voltage defined by equation 3.13 can be measured across the material. If a simple resistive load is attached to the piezoelectric generator, an AC voltage will appear across the load. The average power delivered to load is simply. In reality, a simple resistor is not a very useful load. The voltage should be rectified and conditioned by power management circuit. However, the circuit shown in Figure 3.6 gives an easy and useful calculation of power generation. The voltage and current levels really depend on the physical implementation and the particular electrical load circuit used. In reality, it is quite easy to design a system that produces voltages and currents in the useful range. To harvest an operational voltage, the power management circuit can be used to convert the AC voltage into DC voltage.

### **5.3 Methodology and measurement procedure**

The following section illustrates the methodology used and the measurement procedure followed.

#### **5.3.1. Methodologies**

A sound knowledge of the mechanism of energy harvesting from vibration using piezoelectric material is essential to determine a suitable design methodology. The experimental setup methodology used in this study is shown in Figure 5.8. The mechanical energy from the ambient source is produced by an electrodynamic shaker and it is converted to electrical energy via the piezoelectric material and finally the electricity will be stored [65]. The piezoelectric material PZT-4 been coupled to the electrodynamic shaker, was made to vibrate with it. The electricity is generated immediately when the electrodynamic shaker starts vibrating. The piezoelectric material PZT-4 will then convert the vibrations into electrical energy. The conversion mechanism in the active materials can generate electricity by the use of a relative movement of the mechanical stress and the effect of deformation of the strain used in the mechanical system.

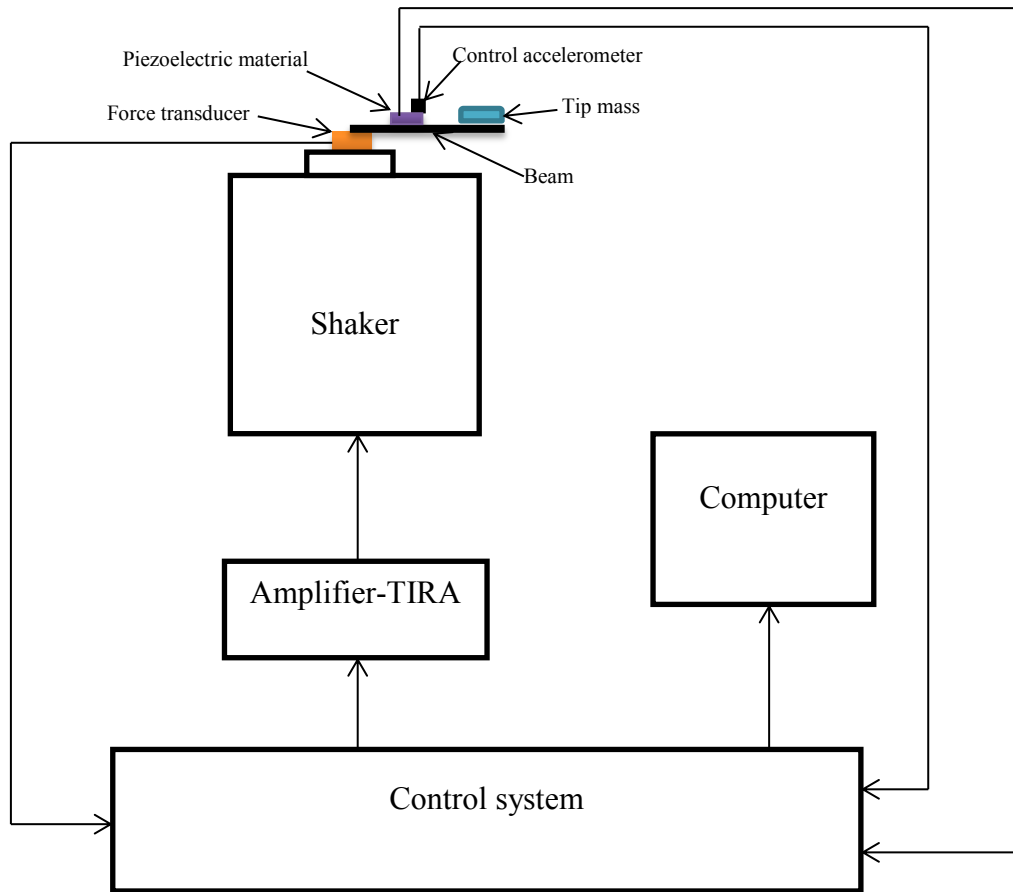


**Figure 5. 8: Schematic diagram of experimental setup**

Methodological experiments must be performed to ensure the correctness of the capacity of the models to predict the quantity of energy produced when they are subjected to variation in vibrations of different amplitudes and frequencies. In order to conduct some initial investigations, an experimental approach was adopted. A prototype cantilever beam harvester was fabricated, and experiments were performed with different components such as accelerometer, force transducer, etc. The purpose of these experiments was to begin to build up some physical intuition in order to better understand this type of device. The objectives were to get a feel for what can be expected regarding the power and voltage, and what (if any) factors should be taken into account in the fabrication and testing of such a prototype cantilever. Because the aim of this thesis is to gather ambient energy from vibration sources and convert it into electrical energy, it was thought that a simple experiment could be undertaken where the fabricated prototype cantilever could be tested with a different range of frequencies by varying velocity. Experimental study was based on the real time measurement

of parameters such as amplitude, frequency of the electrodynamic vibration shaker and the output voltage of the energy harvester.

### **5.3.2. Measurements procedure**

All experiments were performed at room temperature. The measurements were captured by a Puma Vibration Controller and Analysis System shown in Figure 5.5. With scalable hardware and software the Vibration Control and Analysis System combines the simplicity of operation required for production screening with the power and versatility required for testing prototype generators. PUMA incorporates high quality data acquisition and signal generation hardware designed with the latest floating point digital signal processing technology with patented digital vibration control methods. Adaptive control permits PUMA to control and adjust the speed in real time. The study considered the process of energy harvesting as a sequence of conversion steps and all experiment were carried out on an isolated bench to prevent any interference from environment noise and all measurements were performed according to IEEE standards on piezoelectricity, 176-1987 [62]. After compilation of the test, the results obtained were analyzed and presented in diagrams for each measured target level.



## CHAPTER SIX

### EXPERIMENTAL RESULTS AND DISCUSSIONS

---

#### 6.1 Description of the prototype generator

From the literature review, it can be summarized that piezoelectricity based on vibration energy harvesting with piezoelectric material are often configured as a cantilever beam. There is good reason for this. A cantilever results in one of the least stiff structures for a given volume. This means that the cantilever offers both a low resonant frequency and a high average strain in its materials for a given volume. Both of these characteristics are useful for a vibration energy harvester; a high average strain in the piezoelectric layer translates directly into a high power output. From information gleaned from the literature review, it seems that the higher acceleration amplitude vibrations tend to occur at the lower frequency values. Furthermore, as discovered from the power enhancement, if the cantilever is configured to be triangular in shape rather than rectangular, then the maximum tolerable excitation amplitude can be much higher because all of the piezoelectric material can be homogeneously stressed to a value just below the yield stress. In the case of a rectangular cantilever, if the material near the fixed end of the beam is stressed to a value just below the yield stress, the material at the free end is not stressed to the same degree. This means that, for the same size of the device, a triangular shaped beam is capable of outperforming a rectangular shaped beam in terms of power output.

Two design configurations of the cantilever beam were fabricated and used for this study. The first setup, the beam was clamped at one end and the other end was free, i.e., without tip mass. Figure 6.1 illustrates a piezoelectric cantilever beam without a tip mass toward the end.



**Figure 6. 1: Piezoelectric cantilever beam without tip mass**

The second setup, the beam was also clamped at one end and the other end was with a tip mass. Figure 6.2 illustrates the second configurations, piezoelectric cantilever beam with a tip mass at one end of the beam.



**Figure 6. 2: Piezoelectric cantilever beam with tip mass at one end**

Both configurations used PZT-4 attached to a central brass shim (beam) possessing a length of 145 mm, width of 45 mm and a thickness of 0.8 mm. Considering the type of material used for the tip mass, it is known that a greater mass value leads to a piezoelectric material with a lower resonant frequency and higher power output and that it is due to the power density [66]. Therefore, it is conducive to use a material with a high density, since this allows for a greater mass value in a restricted volume. Gold, platinum, lead and silver offer high densities at 21,450; 19,300; 11,340 and 10,500 kg/m<sup>3</sup> respectively. These materials are obviously hard to obtain and too expensive, so steel was a good compromise at 7,930 kg/m<sup>3</sup>. The steel was obtained from some old brackets, which were first cut using a hacksaw and then filed down to size 30 × 45 × 15 mm (Length × Width × Thickness). The weight value of the tip mass was 15 g. On the beam, the tip mass was fixed by using a screw.

## 6.2 Basic mode configuration

In Chapter Three, Figure 3.5 shows the two different mode configuration generally used for piezoelectric material. The labelled number 1, 2, and 3 represents the axes x, y, and z respectively. Normally, the cantilevers operate in the '31 mode', that is, charges are collected in the "3" direction through the electrodes in line with the polarisation of the material, which is conventionally denoted as the "3" direction, and the mechanical strain behaves in the "1" direction. While this is not the most efficient mode of use for a piezoelectric material, the '33 mode', where both the electric field and mechanical strain act in the "3" direction and usually has larger coefficient values (i.e.  $d_{33}$  and  $k_{33}$  are usually larger than  $d_{31}$  and  $k_{31}$ ), use of the '31 mode' enables the benefits brought about by the low stiffness of the cantilever configuration, thus making it more effective compare to '33' mode. Cantilever based piezoelectric energy harvesters work in the following way: when the host structure is put trough to accelerate from a vibration environment (for clarification, acceleration in the "3" direction only is assumed), the inertia of the mass causes the mass to move out of the plane with the host structure. This relative displacement of the mass with the host structure results in curvature of the beam, which causes stress in the "1" direction within the piezoelectric layers. This in turn results in an electrical output through the electrodes of the device in the "3" direction as a consequence of the piezoelectric direct effect.

The prototype generator cantilever based piezoelectric harvester can be arranged either as a unimorph, bimorph, or multi-layer bimorph. In bimorph and multilayer bimorph arrangements the piezoelectric material can be physically wired such that the piezoelectric layers are linked either in parallel or in series. Taking the case of a bimorph as an example, when the piezoelectric layers are subjected to accelerate from a vibration source, the parallel connection requires that the piezoelectric layers are polarized in one direction and the actual polarity charge appears on the outside electrodes of the piezoelectric material. Thereby the outer electrodes are linked together to form one electrical output terminal, and the centre layer creates the other electrical output terminal. The series connection requires that the piezoelectric layers are oppositely poled, such that when acceleration is applied, a charge of one polarity exists on one of the outer electrodes while charge of the opposite polarity exists on the other outer electrode. In this case, each outer electrode becomes an electrical output terminal. For the same size of piezoelectric material, the power output remains the same regardless of whether the device is polled for parallel or series. However, the ratio of current to voltage changes so that for a piezoelectric material poled for series the output voltage is double that of a device poled for parallel, and for a device poled for parallel the output current is double that of a device poled for series [67]. This is because in the parallel case, the surface area of the electrode is able to output current directly to the circuit which is double that of the series case, and in the series case the floating voltage output of each piezoelectric layer are connected in series. Figure 6.3 illustrates the piezoelectric connected as a cantilever beam with PZT polarized in operation.

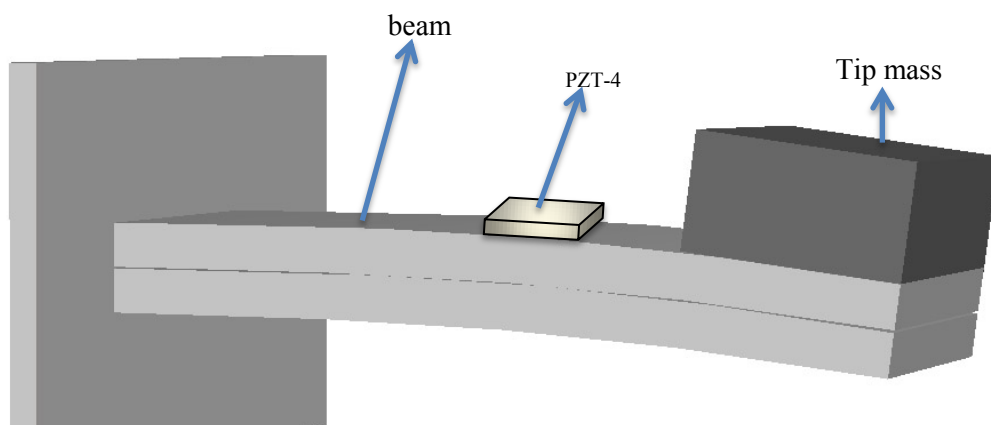


**Figure 6. 3: Piezoelectric cantilever beam with PZT polarized**

### 6.3 Testing of the prototype generator harvester

An easy way of simulating vibration is through the use of an electrodynamic shaker. In order to perform preliminary tests with piezoelectric materials, it was necessary to build a test setup. Once the test setup was built as shown in Figure 5.8, the responses of the electrodynamic shaker TIRA Model, Type TV 56263/LS-340 plus the prototype generator could be captured. The prototype generator is a resonant device, therefore a method of performing a frequency sweep had to be devised so that the resonant frequency could be ascertained and used to power any prototype circuitry that might be developed. However, since a resonance condition can magnify acceleration forces, it is important that the response of the test system itself is flat over the test frequency range between 5 - 200 Hz, and then the response obtained from the harvesting devices can be trusted as a true output of the device.

The form of a piezoelectric prototype generator has a direct effect on its performance harvesting. To conduct a performance study, two tests were conducted to collect the data with two configurations of prototype generator as shown in Figure 6.1 and Figure 6.2. These prototype generators were excited with the same velocity. Figure 6.4 shows the constant velocity for both prototype generators.

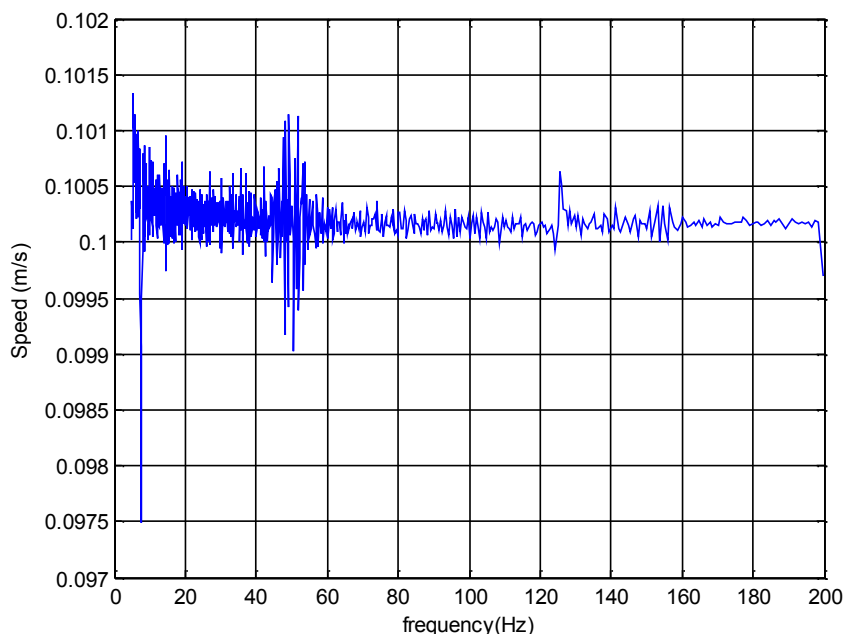


**Figure 6. 4: Graph of constant velocity**

### 6.3.1. Experimental results and discussion of the prototype generator without tip mass

In order to examine the response of the electrodynamic shaker via the prototype generator, an accelerometer was fixed onto the cantilever beam to detect the acceleration of the vibration produced by the electrodynamic shaker. Obviously, while considering the response of the shaker plus the prototype generator, it is also important that the accelerometer itself was used to detect the acceleration of the vibration produced by the shaker and does not have a resonant frequency that falls within the test frequency range. It was also considered that the position of the accelerometer on the cantilever beam might be important. Normally, the accelerometer should be placed close to the end clamped of the cantilever beam as possible, so that it can be used to show the actual acceleration applied to the piezoelectric materials for energy harvesting. The nearest that it was practical to get to this ideal was to mount it onto the top piece of the prototype generator in an optimal test setup so that the output of the accelerometer could be used as part of a feedback loop to calibrate the input to the electrodynamic shaker, so that a constant acceleration could be applied over the test frequency range.

However, this was not available, so it was considered that an open loop system could be used if the frequency response of the electrodynamic shaker plus prototype generator remained flat over the test frequency range. The open loop system depicted was initially devised to obtain both frequency responses; first that for electrodynamic shaker plus prototype generator and second that for piezoelectric materials. The system therefore implements a crude form of voltage control. This value was chosen to make it possible to capture the full output response over the 0 - 200 Hz sweep from both the accelerometer and prototype harvester on the electrodynamic shaker in one test run while maintaining enough resolution to represent the data accurately. In order to make sense of any data collected from the cantilever beam by means of piezoelectric material using this test setup, it was necessary to know what value of voltage output equates to what value of high frequency.

In order to find the resonant frequency, the test was repeated, and various channels were connected to the output of the prototype generator. The results show that the voltage

measured at the point where the beam is at resonance was found to be 4.05 V which, according to the data collected for Figure 6.5, corresponds to a frequency of 108.13 Hz.

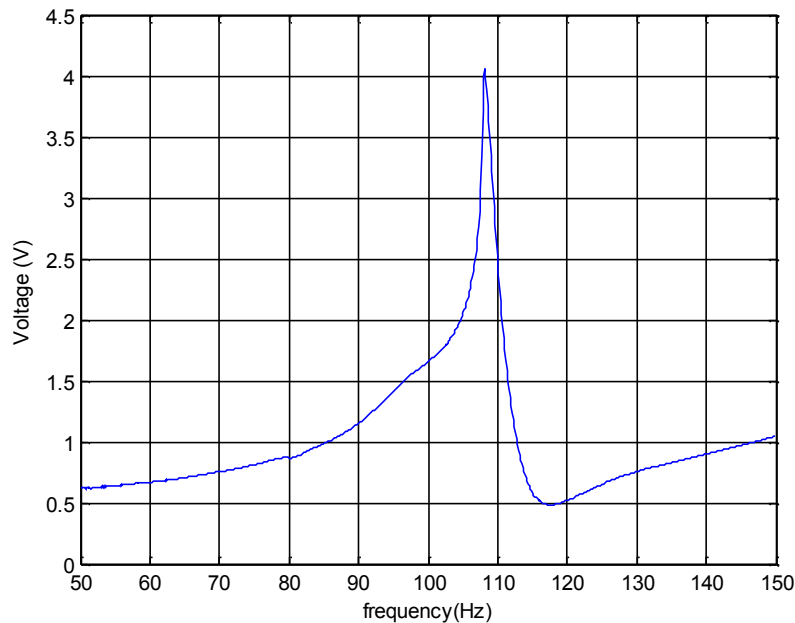


**Figure 6. 5: Graph showing trends of the voltage output generated across the frequency for the first setup**

This graph shows that initially, the value of voltage is high relative to the value of high resonance frequency. This means that the greater portion of voltage available from the AC voltage source will be dropped across the prototype generator internal impedance while the lesser portion of the voltage available will be dropped across the external load resistor. The purpose of finding the resonant frequency of the piezoelectric ceramic material was so that the piezoelectric ceramic material could be characterized in terms of maximum power output. Since the resonance condition dictates maximum displacement of the cantilever beam, maximum power output occurs at the resonant frequency, thus characterisation in terms of the maximum power output should be done. The power output of a piezoelectric energy harvesting material can be most easily characterised through the use of a load resistor. Since a load resistor has no reactive components the power dissipated by the load resistor in watts is easily calculated and wholly represents the useful power output from the generator.

### 6.3.2. Influence of the tip mass on the operation of the energy harvesting

In order to adjust the operation of the harvesting point, another possibility is to add a tip mass to the end of the beam. This is the geometry that has received the most attention in the literature. Adding mass to the end will increase the equivalent mass and increase energy harvested. The structure is composed of a beam length where the piezoelectric material is positioned on a beam length and the mass is positioned along the end of a beam. The material which constitutes the mass elements must have a high density (e.g. tungsten, steel, brass) but for this study for reasons of cost and manufacturing steel was selected as the material of the mass. It is advantageous to increase the total mass of the prototype by adding a tip mass at the end of the cantilever beam. Energy harvested for the same volume of power dissipated is proportional to its mass equivalent due to the energy density of the heat exchanged. The heat generated in piezoelectric materials, the temperature increases while converting the mechanical energy to electrical energy. This is mainly because of dielectric losses in the piezoelectric materials and structural damping losses in the piezoelectric materials. If the high density mass material is already included to create a monolithic structure to start with, this will avoid the necessity of gluing items on later during the experimental set-up.



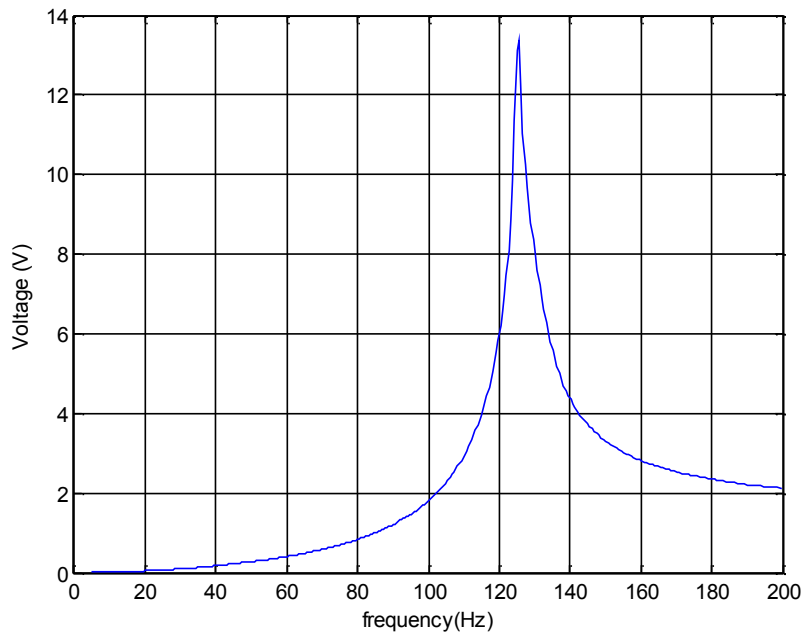


**Figure 6. 6: Graph showing trends of the voltage output generated across the frequency for the second setup**

Figure 6.6 shows the amplitude of the output voltage across the resonance frequency when the tip mass is attached to the beam for the energy harvested. At the same velocity, namely 0.1 m/s, the energy harvesting provides a peak output voltage of 13.35 V at a resonance frequency of 125.5 Hz. As mentioned above, the voltage output increases for this configuration. As the value of tip mass increases, the amplitude of the voltage output will increase because of the high density of the tip mass chosen and the changing of mechanical properties of the structure also affects the resonance frequency (changing dimensions, moving the centre of gravity of the proof mass). The approach requires that the cantilever base clamp be released and re-clamped in a new location along the length of the beam, thereby changing the effective length (and hence frequency). There is no power required to maintain the new resonant frequency. In the next subheading (6.4), the mathematic model is given. It was also shown that the strain distribution has substantially the same shape as that of the setup discussed in the previous sub-section. In this case study, this numerical study observed that the addition of a weight member increases equivalent weight. The addition of a weight member also increases the level of deformation in the piezoelectric material.

In the case study, this numerical study observed that the addition of a weight member increases equivalent weight, the inertial load, and therefore, the power factor. These increases result in an increase of the dissipated power and energy density. By cons, these increases also ensure to increase the level of strain on the piezoelectric materials. It was also shown that the strain distribution has substantially the same shape as that of case 1, of the prototype generator without tip mass, studied in the previous sub-section, and in this case, the result show that the voltage output increasing. This increase is due to the use of a constant thickness beam with a tip mass at the end.

## 6.4 Analytical model of prototype generator relating to the influence of the mass

### 6.4.1. Geometric terms for piezoelectric cantilever beam

Figure 6.7 presents different terms of the piezoelectric cantilever beam.

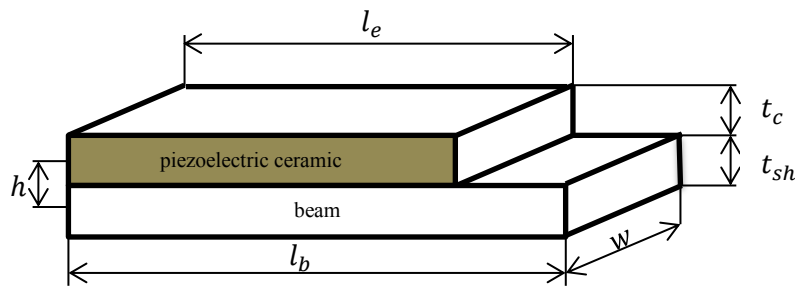


**Figure 6. 7: Geometry terms of the cantilever beam**

Because the piezoelectric bender is a composite beam, an effective moment of inertia and elastic modulus are used. The effective moment of inertia is given by equation 6.1 below.

$$I = \left[ \frac{wnt_c^3}{12} + wnt_c b^2 \right] + \frac{\eta_s w t_{sh}^3}{12} \quad 6.1$$

Where:

$w$  Width of the beam.

$b$  The distance from the centre of the beam to the centre of piezoelectric ceramic.

$\eta_s$  The ratio of the piezoelectric material constant to that of the centre beam ( $\eta_s = Y_c/Y_{sh}$

where  $Y_c$  is the Young's modulus for the piezoelectric ceramic and  $Y_{sh}$  is the Young's modulus for the centre beam).

$t_{sh}$  The thickness of the centre beam.

$t_c$  The thickness of the piezoelectric ceramic.

$n$  Indicate the number of piezoelectric ceramic.

The elastic constant for the piezoelectric ceramic is then used in conjunction with the effective moment of inertia shown by equation 6.1. The different Young's modulus of the centre beam is accounted for by the term  $\eta_s$  in the moment of inertia [68].

Because the piezoelectric constitutive equations deal directly with stress and strain, it is most convenient to use them as the state equations for the dynamic system rather than force and displacement. However, in order to derive state equations in terms of stress and strain for the piezoelectric bender mounted as a cantilever beam as shown in Figure A.2, two geometric terms need to be defined. The first relates vertical force to average stress in the piezoelectric material, and the second relates tip deflection of the beam to average strain in the piezoelectric material.

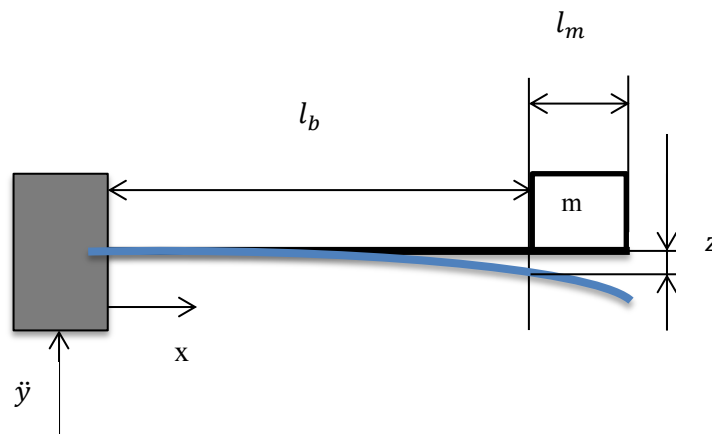


**Figure 6. 8: Schematic of piezoelectric bender**

When purchased, the piezoelectric benders are covered with an electrode. The electrode can be easily etched away making the only the portion of the beam covered by the electrode

active as a piezoelectric material. Referring to Figure 6.7, it will be assumed that the electrode length ( $l_e$ , not shown in the Figure 6.8) is always equal to or less than the length of the beam ( $l_b$  is showing in the Figure 6.8). The stress and strain values of interest, and those used as state variables are the average stress and strain in the piezoelectric material that is covered by an electrode. An expression for the average stress in the piezoelectric material covered by the electrode (hereafter referred to simply as stress) is given by equation 6.2.

$$\sigma = \frac{1}{l_e} \int_0^{l_e} \frac{M(x)b}{I} dx \quad 6.2$$

Where:

$\sigma$  Stress.

$x$  The distance from the base of the beam

$M(x)$  The moment in the beam as a function of the distance ( $x$ ) from its base.

The moment,  $M(x)$ , is given by equation 6.3.

$$M(x) = m(\ddot{y} + \ddot{z})(l_b + \frac{1}{2}l_m - x) \quad 6.3$$

Where:

$z$  The vertical displacement of the beam at the point where the mass attaches with respect to the base.

$\ddot{y}$  The input vibration in term of acceleration.

$l_m$  The length of the mass.

Substituting equation 6.3 in to equation 6.2 yields the expression in 6.4.

$$\sigma = m(\ddot{y} + \ddot{z}) \frac{b(2l_b + l_m - l_e)}{2I} \quad 6.4$$

The vertical force term in equation 6.4 is simply  $m(\ddot{y} + \ddot{z})$ . Therefore, let us define  $b^{**}$  as shown in equation 6.5.

$$b^{**} = \frac{2I}{b(2l_b + l_m + l_e)} \dot{y} \quad 6.5$$

$b^{**}$  Then relates vertical force to stress ( $\sigma$ ), and  $= \frac{m(\ddot{y} + \ddot{z})}{b^{**}}$ .

In order to derive the term relating deflection at the point where the beam meets the mass as shown in Figure 6.7 to average strain in the piezoelectric material covered by the electrode (simply strain hereafter), consider the Euler beam equation shown as 6.6.

$$\frac{d^2z}{dx^2} = \frac{M(x)}{Y_C I} \quad 6.6$$

By substituting equation 6.3 into equation 6.6, yields equation 6.7.

$$\frac{d^2z}{dx^2} = \frac{1}{Y_C I} m(\ddot{y} + \ddot{z})(l_b + \frac{1}{2}l_m - x) \quad 6.7$$

Integrating to obtain an expression for the deflection term ( $z$ ) yields:

$$z = \frac{m(\ddot{y} + \ddot{z})}{Y_C I} \left[ \left( l_b + \frac{1}{2}l_m \right) \frac{x^2}{2} - \frac{x^3}{6} \right] \quad 6.8$$

At the point where the beam meets the mass (at  $x = l_b$ ), the expression for  $z$  becomes:

$$z = \frac{m(\ddot{y} + \ddot{z})l_b^2}{2Y_C I} \left[ \left( \frac{2}{3}l_b + \frac{1}{2}l_m \right) \right] \quad 6.9$$

Finally, realizing that strain is equal to stress over the elastic constant,  $S = \sigma/Y$ , and that stress can be expressed as in equation 6.4, strain can be written as shown below:

$$S = \frac{m(\ddot{y} + \ddot{z})b}{2Y_C I} (2l_b + l_m - l_e) \quad 6.10$$

Rearranging equation 6.10, the force term,  $m(\ddot{y} + \ddot{z})$ , can be written as shown in equation 6.11.

$$m(\ddot{y} + \ddot{z}) = \frac{2Y_C I}{b(2l_b + l_m - l_e)} S \quad 6.11$$

Substituting equation 6.11 into equation 6.9 yields:

$$z = S \frac{l_b^2 \left( 2l_b + \frac{3}{2} l_m \right)}{3b(2l_b + l_m - l_e)} \quad 6.12$$

Let us define  $b^*$  as shown in equation 6.13.  $b^*$  then relates strain to vertical displacement, or  $z = S/b^*$ .

$$b^* = \frac{3b(2l_b + l_m - l_e)}{l_b^2 \left( 2l_b + \frac{3}{2} l_m \right)} \quad 6.13$$

#### 6.4.2. Dynamic model of piezoelectric cantilever beam

A convenient method of modelling piezoelectric materials such that system equations can be easily developed is to model both the mechanical and electrical portions of the piezoelectric system as circuit elements. The piezoelectric coupling is then modelled as a transformer [69]. Figure 6.7 shows the circuit model for a piezoelectric material. Note also that no electric load is applied to the system.

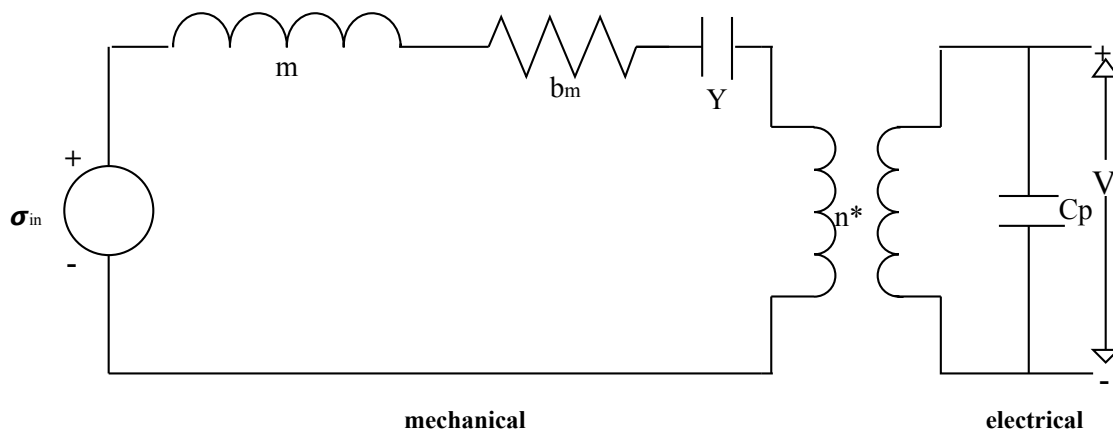


**Figure 6. 9: Circuit representation of piezoelectric bimorph**

The across variable (variable acting across a piezoelectric material) on the electrical side is voltage (V) and the through variable (variable acting through a piezoelectric material) is current (i) [70]. The across variable on the mechanical side is stress ( $\sigma$ ) and the through variable is a string (S). The system equations can then be obtained by simply applying Kirchoff's Voltage Law (KVL) and Kirchoff's Current Law (KCL).

However, first the stress / strain relationships of circuit elements on the mechanical side need to be defined. It is easier to use stress and strain as variables rather than force and tip displacement because the piezoelectric charge coefficient (d) relates to stress and strain. As will be shown later, the strain becomes the state variable rather than the more commonly used displacement in the equations of motion.

$\sigma_{in}$  is an equivalent input stress. In other words, it is the stress developed as a result of the input vibrations. The mass (m) attached to the end of the cantilever beam is shown as an inductor or inertial term. The stress “across” this element is the stress developed as a result of the mass flexing the beam. Equation 6.4 gives the stress resulting from both the input element,  $\sigma_{in}$ , and the inertial element, m. Thus, the relationships of these two elements are given in equations 6.14 and 6.15.

$$\sigma_{in} = \frac{m}{b^{**}} \ddot{y} \quad 6.14$$

$$\sigma_m = \frac{m}{b^{**}} \ddot{z} \quad 6.15$$

Where  $b^{**}$  is the geometric constant relating average bending stress to force at the beam’s end.

However, the preferred state variable is strain S, rather than displacement z. Substituting strain for displacement in 6.15 using the relationship from equation 6.12 and 6.13 yields the stress / strain relationship of the inertial element, m, in equation 6.16.

$$\sigma_m = \frac{m}{b^* b^{**}} \ddot{S} \quad 6.16$$

Where  $b^*$  is the geometric constant relating average strain to displacement at the beam’s end.

The resistive element in Figure 6.9 represents damping, or mechanical loss. The damping coefficient  $b_m$ , relates stress to tip displacement z. Therefore, it should be noted that the units of the piezoelectric damping coefficient  $b_m$  of this model are  $\text{Ns/m}^3$  rather than the more conventional  $\text{Ns/m}$ . The stress / strain relationship for the piezoelectric damping coefficient,  $b_m$ , becomes:

$$\sigma_{bm} = \frac{b_m}{b^*} \ddot{S} \quad 6.17$$

Finally, the stiffness term (Y), relating stress to strain is represented as a capacitor and labelled with the elastic constant.  $C_p$  is the capacitance of the bimorph. The stress / strain relationship of this element is simply Hooke's law, shown here as equation 6.18.

$$\sigma_Y = Y_c S \quad 6.18$$

The transformer relates stress ( $\sigma$ ) to electric field (E) at zero strain, or electrical displacement (D) to strain (S) at zero electric field. So the equations for the transformer follow directly from the two mathematically linearized equations 4.1 and 4.2 in chapter four, and are:

$$D_t = -dY_c S \quad 6.19$$

$$\sigma_t = -dY_c E \quad 6.20$$

The equivalent turns ratio ( $n^*$ ) for the transformer is then  $-dY$ . The state variables, however, are current  $\dot{q}$  and voltage  $V$ . Noting that  $q = nl_e w D$  and that  $V = E t_c$  the equations for the transformer can be rewritten as:

$$\dot{q}_t = -dY_c n l_e w \dot{S} \quad 6.21$$

$$\sigma_t = \frac{-dY_c}{t_c} V \quad 6.22$$

Note that the expressions in equations 6.21 and 6.22 assume that the piezoelectric layers are all wired in parallel. If any layers that are wired in series are considered a single layer, the model will still hold. For example, if the bender is a two layer bimorph wired in series, the number of layers in the calculations should be one, and the piezoelectric thickness ( $t_c$ ) used should actually be the sum of the thickness of the two layers.



Once the circuit in Figure 6.7 has been defined and the relationship between the physical beam and the circuit elements on the “mechanical” side of the circuit has been specified, system equations can be developed using Kirchhoff’s Voltage Law to yield the following equation:

$$\sigma_{in} = \sigma_m + \sigma_{bm} + \sigma_t \quad 6.23$$

Substituting equations 6.14, 6.16, 6.17, 6.18, and 6.22 into 6.23 and rearranging terms yields the third order equation shown as 6.24, which describes the mechanical dynamics of the system with an electrical coupling term.

$$\ddot{S} = -\frac{Yb^*b^{**}}{m}S - \frac{b_m b^{**}}{m}\dot{S} + \frac{dY_c b^*b^{**}}{t_c m}V + b^*\ddot{y} \quad 6.24$$

The combined term  $Yb^*b^{**}$  has units of force / displacement and relates vertical force to tip deflection. This is commonly referred to as the effective spring constant. Letting  $k_{sp}$  be the effective spring constant, and substituting  $k_{sp} = Yb^*b^{**}$  into equation 6.24 yields the simpler and more familiar expression in equation 6.25.

$$\ddot{S} = -\frac{k_{sp}}{m}S - \frac{b_m \dot{b}}{m}\dot{S} + \frac{k_{sp}d}{mt_c}V + b^*\ddot{y} \quad 6.25$$

Where  $k_{sp}$  is equivalent spring constant of cantilever beam.

Equation 6.25 forms a portion of the complete dynamic model. Applying KCL to the electrical side of the circuit in Figure 6.24 yields the rest of the model. Equation 6.26 is the very simple result of applying KCL to the electrical side of the equivalent circuit.

$$\dot{q}_t = \dot{q}_{Cp} \quad 6.26$$

Where:

$\dot{q}_t$  The current through the transformer as defined in equation 6.21.

$\dot{q}_{Cp}$  The current through the capacitor  $C_p$ .

The capacitance of the piezoelectric material is  $C_p = \frac{n\epsilon w l_e}{t_c}$ . Substituting equation 6.21 into 6.26, using the long expression for  $C_p$ , and rearranging terms yields the equation shown as 6.27.

$$\dot{V} = \frac{-dY_c t_c}{\varepsilon} \dot{S} \quad 6.27$$

Where:

$V$  Voltage at the output.

$t_c$  Thickness of a single layer of the piezoelectric material.

Equations 6.25 and 6.27 constitute the dynamic model of the system. They can be rewritten in state space form as shown in equation 6.28.

$$\begin{bmatrix} \dot{S} \\ \ddot{S} \\ \dot{V} \end{bmatrix} = \begin{bmatrix} 0 & 1 & 0 \\ -\frac{k_{sp}}{m} & -\frac{b_m b^{**}}{m} & \frac{k_{sp} d}{m t_c} \\ 0 & -\frac{d Y_c t_c}{\varepsilon} & 0 \end{bmatrix} \begin{bmatrix} S \\ \dot{S} \\ V \end{bmatrix} + \begin{bmatrix} 0 \\ b^* \\ 0 \end{bmatrix} \ddot{y} \quad 6.28$$

As noted previously, no electrical load has been applied to the system. The right side of Figure 6.7 is an open circuit.

### 6.5 Validation of the two approaches to design of the cantilever beam

In this study, two approaches to configuration of the prototype generator were conducted to collect the data. The results obtained on different configurations shows that there is a good correlation between the predicted model of Roundy et al. [24] and the experimental results to experimentals results for this study. The output voltage of both configuration prototype generators, namely, the first and second setup, is proportional to the tip mass attached to the beam and this should be maximized provided size and deformation stresses are not exceeded. We can adjust this geometry during the operation to perform the energy harvesting. It has been determined that the harvesting for the peak output voltage correspond at one resonance frequency. The vibration source is harvested from mechanical energy to electrical energy through the incorporation of the piezoelectric material on the cantilever beam. These items (cantilever beam) follow the dimensions defined above; a length of 140 mm, a thickness of 0.8 mm and a width of 45 mm. From the tip mass selected it should be noted that the effect of length of the beam on the natural frequency is the same (increase in the length of the beam

causes decrease in the value of the natural frequency). Also the amplitude of vibrations has higher values with an increase in the length of the beam which finally causes higher amplitude of the output voltage. Hence, by increasing the mass of the beam by a tip mass, the resonant frequency of the beam-mass system decreases. Coefficient does not depend on the beam length; however by increasing beam length, the term decreases sharply and as a result the resonant frequency is decreased as the beam length increases.

Figure 6.8 and Figure 6.9 show the time results for the cantilever beam to reach high voltage for the two designs configurations. As evident in the graphs, the second approach made more time compared to the first setup to attend the peak voltage output.

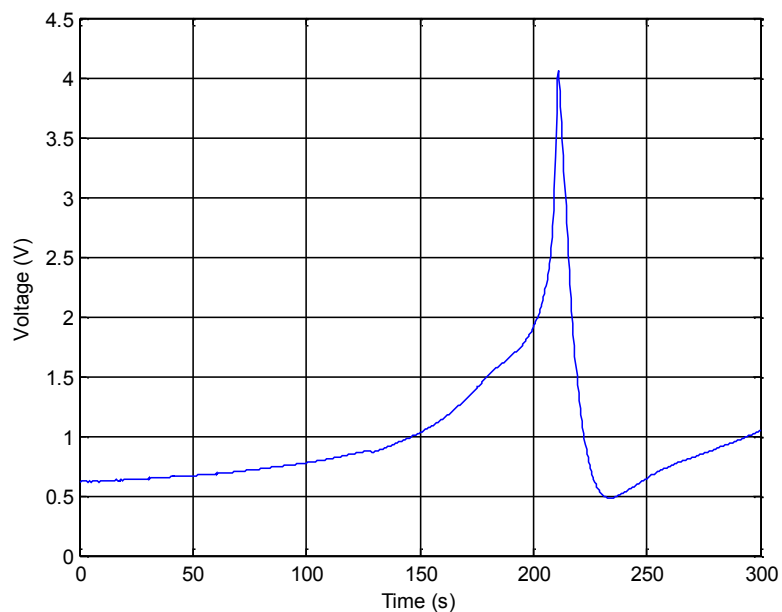


**Figure 6. 10: Time for output voltage for first setup**

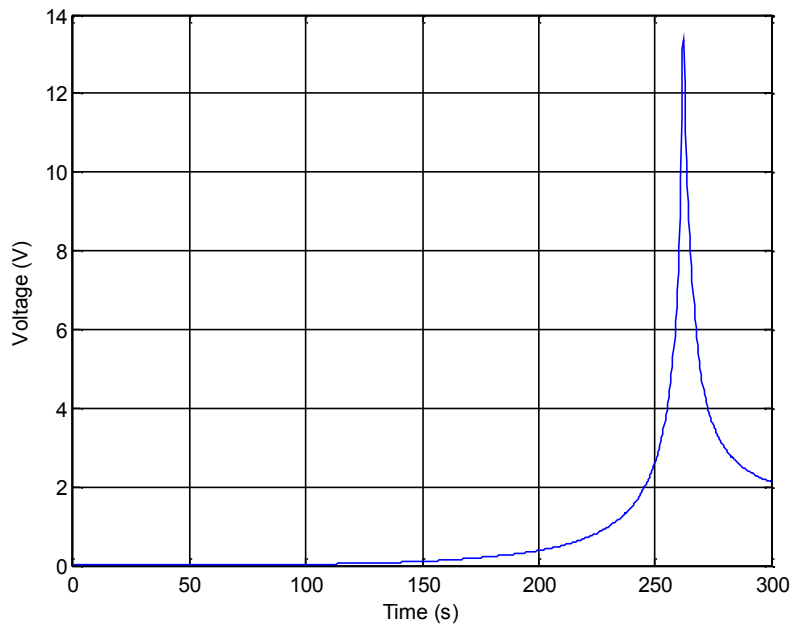


**Figure 6. 11: Time for output voltage for second setup**

## CHAPTER SEVEN

### CONCLUSIONS AND RECOMMENDATIONS

---

#### 7.1 Conclusions

This dissertation presents a study of energy harvesting from vibration using the piezoelectric material, PZT-4. Piezoelectric vibration energy harvesting is one of three common conversion techniques used to harness power. It presents the easiest method, in which vibrations from structures are converted into electrical energy by using a piezoelectric material. It is not complex and does not have compound geometries. The conversions derived from piezoelectricity are the most basic type of prototype generator fabricated and can be used in applications related to the force and impact. One major advantage of this conversion principle is its particular adaptation to micro-engineering, since there exist several different processes for piezoelectric film deposition. Piezoelectric conversion has the capacity to produce electrical current at high voltages, and this electrical current can be utilized in powering some devices or stored for future usage.

Focusing on the objectives in the current study, we have designed, developed and tested a comprehensive prototype generator that can harvest available vibration in the form of mechanical energy and convert it to electrical energy by providing the estimate of output voltage. Two types of setup were experimented with, and had their system performance data recorded using PUMA control systems software and analyzed. The first setup was the prototype generator without tip mass toward the end of a cantilever beam while the second setup was the prototype generator with a tip mass situated at the end of a cantilever beam.

As results from these two setups, the dimensions of the cantilever beam were defined, being a length of 145 mm, a width of 45 mm and a thickness of 0.8 mm. The first set up was determined as energy harvesting provided a peak output voltage of 4.05 V at 108.13 Hz resonance frequency. For the second setup, the output voltage measured was 13.35 V at 125.5 Hz resonance frequency. From the above results, the amplitude of the output voltage, the

impact of a tip mass on the resonance frequency of the energy harvester was found. It can be seen that the first setup has the peak output voltage at a lower frequency compared to the second setup which has a peak output voltage at a higher frequency. This means that the prototype generator with a tip mass toward the end of a cantilever beam, the resonance frequency decreased and the amplitude of voltage increased as compared to the prototype generator without a tip mass at the end of a cantilever beam. The tip mass produced the quantity of harvested energy and then the output voltage of the generator at resonance frequency is proportional to the tip mass that is glued to the cantilever beam. This should be maximized on condition that strain constraints and size are not surpassed.

The power generated by the piezoelectric materials performance under resonant low frequency excitation is governed by the elastic compliance and piezoelectric constant rather than the mechanical quality factor. The second setup could be an attractive choice and the output power is sufficient to power wireless sensors. This prototype model offers a relationship to design other devices for evolving energy harvesting systems by providing assistance in identifying the size and magnitude of vibration necessary to bring about the level of desired power output generation. The benefits and the advances of energy harvesting by vibration for wireless sensors and low power electronics are helping to make the technology very bright in the future.

## **7.2 Recommendations for future work**

The present work investigated energy harvesting by piezoelectric materials to convert mechanical energy to electrical energy. The power generated by a piezoelectric material cannot be directly used by other electric devices, and therefore some electric interface is necessary for the energy harvesting system to ensure the voltage compatible with electric load or energy storage element. There are many different schemes of the electric interface developed for energy harvesting such as AC voltage to a DC voltage rectifier, voltage doubler, etc. As noted previously, an equivalent circuit of the output voltage of the prototype generator is needed to rectify and convert the alternating current (AC) voltage into direct current (DC) voltage. This DC voltage output of the equivalent circuit is also able to power various electronic devices. Future work might consider using a power management

equivalent circuit to store and convert the electrical energy in the form of AC voltage harvested from the piezoelectric materials to DC voltage. The power management equivalent circuit must fulfil two main functions. The first function is that the power management equivalent circuit needs to store the electrical energy harvested from the piezoelectric materials. The second function is that after the energy storage has reached a suitable level, the power management equivalent circuit needs to provide a stable DC output. The power management equivalent circuit should consist of a capacitor to store the electrical energy and a voltage regulator. Future studies should investigate energy harvesting operation under power management to store the charge output in a capacitor and to regulate the AC voltages.

## REFERENCES

---

- [1] T. Armontroug, "Energy harvesting applications are everywhere," *Linear Technology, RTC Group*, pp. 1-5, 2009.
- [2] R. M. Manisha, S. N. Namrata, and H. K. Abhyankar, "Micro energy harvesting for biomedical application: A Review," *IEEE Electronics Computer Technology*, vol. 03, pp. 1-5, 2011.
- [3] S. K. Heung, K. Joo-Hyong and K. Jaehwan, "A review of piezoelectric energy harvesting based on vibration," *International Journal of Precision Engineering and Manufacturing*, vol. 12, pp. 1129-1141, 2011.
- [4] S. Roundy, P. K. Wright and J. Rabaey, "A study of low level vibrations as a power source for wireless sensor nodes," *Computer Communications*, vol. 26, pp. 1131-1144, 2003.
- [5] S. P. Beeby, M. J. Tudor and N. M. White, "Energy harvesting vibration sources for microsystems applications," *Measurement Science and Technology*, vol. 17, pp. 175-195, 2006.
- [6] S. P. Beeby, R. N. Torah, M. J. Tudor, P. G. Jones, T. O. Donnell and C. R. Saha, "A micro electromagnetic generator for vibration energy harvesting," *Journal of Micromechanics and Microengineering*, vol. 17, pp. 1257-1265, 2007.
- [7] W. J. Li, T. C. H. Ho, G. M. H. Chan, P. H. W. Leong and H. Y. Wong, "Infrared signal transmission by a laser-micromachined, vibration-induced power generator," *In Circuits and Systems, IEEE Proceedings Midwest*, vol. 01, pp. 236-239, 2000.
- [8] C. B. Williams, C. Shearwood, M. A. Harradine, P. H. Mellor, T. S. Birch and R. B. Yates, "Development of an electromagnetic micro-generator," *IEEE Procedure G-Circuits, Devices and Systems*, vol.148, pp. 337-342, 2001.
- [9] Q. Zhang and E. S. Kim, "Energy harvesters with high electromagnetic conversion efficiency through magnet and coil arrays," *IEEE, MEMS 2013, Taipei, Taiwan*, vol. 01, pp. 110-113, 2013.



- [10] Ö. Zorlu and H. Kùlah, "A MEMS-based energy harvester for generating energy from non-resonant environmental vibrations " *Sensors and Actuators A: Physical*, vol. 201, pp. 124-134, 2013.
- [11] P. Wang, H. Liu, X. Dai, Z. Yang, Z. Wang and X. Zhao, "Design, simulation, fabrication and characterization of a micro electromagnetic vibration energy harvester with sandwiched structure and air channel," *Microelectronics Journal*, vol. 43, pp. 154-159, 2012.
- [12] Y. Chiu and C. F. Chang, "Modelling and analysis of a DC electrostatic vibration-to-electricity micro power generator," *Power MemS*, pp. 1-4, 2010.
- [13] A. M. Paracha, P. Basset, D. Galayko, A. Dudka, F. Marty and T. Bourouina, "Mems DC/DC converter for 1d and 2d vibration-to-electricity power conversion,," *Actuators and Microsystems Solid-State Sensors, IEEE Transducers*, pp. 2098-2101, 2009.
- [14] C. Lee, Y. M. Lim, B. Yang, R. K. Kotlanka, C. H. Heng and He. J.H., "Theoretical comparison of the energy harvesting capability among various electrostatic mechanisms from structure aspect," *Sensors and Actuators A: Physical*, vol. 156, pp. 208-216, 2009.
- [15] F. Cottone, P. Basset, R. Guillemet, D. Galayko, F. Marty and T. Bourouina, "Bistable multiple-mass electrostatic generator for low-frequency vibration energy harvesting," *IEEE, MEMS*, pp. 861-864, 2013.
- [16] A. Kempitiya, D. A. Borca-Tasciuc and M. M. Hella, "Low power ASIC for microwatt electrostatic energy harvesters," *Industrial electronics, IEEE transactions on Very Large Scale Integration (VLSI) Systems*, vol.12, pp. 5639-5647, 2012.
- [17] D. Galayko, R. Guillemet, A. Dudka and P. Basset, "Comprehensive dynamic and stability analysis of electrostatic vibration energy harvester (E-VEH)," *IEEE, Transducers*, vol. 11, pp. 2382-2385, 2011.
- [18] Y. Chiu, C. T. Kuo and Y. S. Chu, "Design and fabrication of a micro electrostatic vibration-to-electricity energy converter," *DTIP of MEMS & MOEMS*, pp. 1-6, 2006.
- [19] S. N. Chen, G. J. Wang and M. C. Chien, "Analytical modelling of piezoelectric vibration-induced micro power generator," *Mechatronics*, vol. 16, pp. 379-387, 2006.

- [20] C. Lu, C. Y. Tsui and W. H. Ki, "Vibration energy scavenging system with maximum power tracking for micro power applications," *IEEE Transactions on Very Large Scale Integration (VLSI) Systems*, vol. 19, pp. 2109-2119, 2011.
- [21] N. Elvin, A. Elvin and D. H. Choi, "A self-powered damage detection sensor," *Journal of Strain Analysis*, vol. 38, pp. 115-124, 2003.
- [22] H. A. Sodano, G. Park and D.J. Inman, "Estimation of electric charge output for piezoelectric energy harvesting," *Journal of Strain Analysis*, vol. 40, pp. 49-58, 2004.
- [23] J. H. Qiu, H. L. Ji and H. Shen, "Energy harvesting and vibration control using piezoelectric elements and a nonlinear approach," *IEEE International Symposium on the Application of Ferroelectrics*, vol. 18, pp. 1-8, 2009.
- [24] S. Roundy, P. H. Wright and J. M. Rabaey, "Energy scavenging for wireless sensor networks with special focus on vibrations, " Boston, MA ; *Kluwer*, 2004.
- [25] E. S. Leland and P. K. Wright, "Resonance tuning of piezoelectric vibration energy scavenging generators using compressive axial preload " *Smart Materials and Structures*, vol. 15, pp. 1413-1420, 2006.
- [26] C. Eichhorn, F. Golschmidtboeing and P. Woais, "Bidirectional frequency tuning of a piezoelectric energy converter based on a cantilever beam," *journal of Micromechanics and Microengineering*, vol. 19, pp. 1-7, 2009.
- [27] V. R. Challa, M. G. Prasad, Shi. Y. and F. T. Fisher, "A vibration energy harvesting device with bidirectional resonance frequency tunability," *Smart Materials and Structures*, vol. 17, pp. 1-12, 2008.
- [28] S. Roundy, "On the effectiveness of vibration-based energy harvesting," *Journal of Intelligent Material Systems and Structure*, vol. 16, pp. 809-823, 2005.
- [29] C. Peters, D. Maurath, W. Schock, F. Mezger and Y. Manoli, "A closed-loop wide-range tunable mechanical resonator for energy harvesting systems," *journal of Micromechanics and Microengineering*, vol. 19, pp. 1-11, 2009.
- [30] H. B. Fang, J. Q. Liu, Z. Y. Xu, L. Dong, L. Wang and D. Chen, "Fabrication and performance of MEMS-based piezoelectric power generation for vibration energy harvesting," *Microelectron. J.*, vol. 37, pp. 1280-1284, 2006.

- [31] J. Q. Liu, H. B. Fang, Z. Y. Xu, X. H. Mao, X. C. Shen and D. Chen, "A MEMS-based piezoelectric power generator array for vibration energy harvesting," *Microelectron. J.*, vol. 39, pp. 802-806, 2008.
- [32] M. Renaud, K. Karakaya, T. Sterken, P. Fiorini, C. V. Hoof, and R. Puers, "Fabrication, modeling and characterization of MEMS piezoelectric vibration harvester," *Sensors and Actuators A: Physical*, vol.37, pp. 380-386, 2008.
- [33] P. Murali, M. Marzencki, B. Belgacem, F. Calame and S. Basrour, "Vibration energy harvesting with PZT micro device," in *Procedia Chemistry*, vol. 1, pp. 1191-1194, 2009.
- [34] W. L. Zhou, G. R. Penamalli and L. Zuo, "An efficient vibration energy harvester with a multi-mode dynamic magnifier," *Smart Materials and Structures*, vol. 21, 2012.
- [35] R. Patel, S. McWilliam and A. A. Popov, "A geometric parameter study of piezoelectric coverage on a rectangular cantilever energy harvester," *Smart Materials and Structures*, vol. 20, 2011.
- [36] N. S. Lewis and G. Crabtree, "Basic research needs for solar energy utilization," *Report of the Basic Energy Sciences Workshop on Solar Energy Utilization. US Department of Energy, Office of Basic Energy Science , Washington, DC, April 18-21, 2005.*
- [37] M. Roeb and H. Müller-Steinhagen, "Concentrating on solar electricity and fuels," *Sciences*, vol. 329, pp. 773-774, 2010.
- [38] Chen Gang, "Theoretical Efficiency of Solar Thermoelectricity Energy Generator," *Journal of Applied Physics*, vol. 109, pp. 1-8, 2011.
- [39] M. A. Green, K. Emery, Y. Hishikawa and W. Warta, "Solar cell efficiency tables (version 37)," *Progress in Photovoltaics: Research and Applications*, vol. 19, pp. 84-92, 2011.
- [40] C.-T. Chen, R. A. Islam and S. Priya, "Electric energy generator," *IEEE Transactions on Ultrason Ferroelectric Frequency Control*, vol. 53, pp. 656-661, 2006.
- [41] D. Rancourt, A. Tabesh and L. G. Fréchette, "Evaluation of centimeter-scale micro wind mills: aerodynamics and electromagnetic power generation," *7th international*

- workshop on micro and nanotechnology for power generation and energy conversion applications (PowerMEMS 2007)*, Freiburg, Germany, Nov 28-29, 2007.
- [42] S. Pobering and N. Schwesinger, "Power supply for wireless sensor systems," *IEEE Sensors 2008*, pp. 685-688, Lecce, Italy, Oct 26-29, 2008.
- [43] C. C. Federspiel and J. Chen, "Air-powered sensor," *In: 2nd IEEE International Conference on Sensors (Sensors 2003)*, vol. 01, pp. 22-25, Toronto, Canada, Oct 22-24, 2003.
- [44] S. O. Kassap, "Thermoelectric effects in metals," *Thermocouples*, [Online], Available: [Kassap3.usask/samples/Thermoelectric-Seebeck.pdf](http://Kassap3.usask/samples/Thermoelectric-Seebeck.pdf), 2001.
- [45] Y. K. Tan, K. Y. Hoe and S. K. Panda, "Energy harvesting using piezoelectric igniter for self-power radio frequency (RF) wireless sensor," *IEEE International Conference on Industrial Technology*, 2006.
- [46] A. Valenzuela, "Batteryless energy harvesting for embedded designs," [Online], Available: <http://www.embedded.com/design/mcus-processors-and-socs/4008326/Batteryless-energy-harvesting-for-embedded-designs>, 2009.
- [47] G. Park, T. Rosing, M. D. Todd, C. R. Farrar and W. Hodgkiss, "Energy harvesting for structural health monitoring sensor networks," *Journal of Infrastructure Systems*, vol. 14, pp. 64-79, 2008.
- [48] S. R. Anton and H. A. Sodano, "A review of power harvesting using piezoelectric materials (2003-2006)," *Smart Materials and Structures*, vol. 16, pp. 1-21, 2007.
- [49] C. B. Williams and R. B. Yates, "Analysis of micro-electric generator for microsystems," *Sensors and Actuators A: Physical*, vol. 52, pp. 8-11, 1996.
- [50] N. G. Stephen, "On energy harvesting from ambient vibration," *Journal of Sound and Vibration*, vol. 293, pp. 409-425, 2006.
- [51] T. J. Kazmierski and S. Beeby, "Energy harvesting system: principles modelling and application," *New York: Springer*, pp. 1-77, 2011.
- [52] S. Meninger, J.O. Mur-Miranda, R. Amirtharajah, A. P. Chandrakasan and J.H. Lang, "Vibration-to-electric energy conversion," *IEEE Transactions on the Very Large Scale Integration (VLSI) Systems*, vol. 09, pp. 64-76, 2001.

- [53] G. Despesse, T. Jager, J-J. Chaillout, J-M. Léger and S. Basrour, "Design and fabrication of a new system for vibration energy harvesting," *IEEE, Research in Microelectronics and Electronics*, vol. 01, pp. 225-228, 2005.
- [54] H. A. Sodano, D. J. Inman and G. Park, "Generation and storage of electricity from power harvesting devices," *Journal of Intelligent Material Systems and Structures*, vol. 16, pp. 67-75, 2005.
- [55] K. A. Cook-Chennault, N. Thambi and A. M. Sastry, "Powering MEMS portable devices: A Review of non-regenerative and regenerative power supply systems with special emphasis on piezoelectric energy harvesting systems," *Smart Materials and Structures*, vol. 17, 2008.
- [56] D. A. Skoog, H. F. James and S. R. Crouch, "Principles of instrumental analysis " 6<sup>th</sup> edition, Belmont, CA: Brooks/Cole Cengage Learning pp. 09, 2007.
- [57] S. Katzir, "The beginnings of piezoelectricity: A Study in Mundane Physics," *Springer Dordrecht, Netherlands*, vol. 246, pp. 15-64, 2006.
- [58] A. Ballato, "Piezoelectricity: history and new thrusts," *IEEE ultrasonics symposium, San Antonio, TX, USA*, vol. 01, pp. 575-583, Nov 3-6, 1996.
- [59] "Piezo Systems, Inc. History of Piezoelectricity," <http://www.piezo.com/tech4history.html> visited this page 2 times. Last visit: 2013/07/30.
- [60] G. W. Taylor, "Piezoelectricity " *Ferroelectricity and related phenomena*, New-York: Gordon and Breach Science Publishers, vol. 04, 1985.
- [61] H. Kawai, "The Piezoelectricity of Poly (Vinylidene Fluoride)," *Japanese Journal of Applied Physics*, vol. 08, p. 975, 1969.
- [62] "IEEE Standard on Piezoelectricity," *ANSI/ IEEE Standard 176-1987*.
- [63] D. G. Kim, S. N. Yun, Y. B. Ham and J. H. Park, "Energy harvesting strategy using piezoelectric element driven by vibration method," *Wireless Sensor Network*, vol. 02, pp. 100-107, 2010.
- [64] "Steminc, Steiner and Martin, Inc," [http://www.steminc.com/piezo/PZ\\_property.asp](http://www.steminc.com/piezo/PZ_property.asp). visited this page 3 times. Last visit: 2014/06/24.

- [65] D. Guyomar and M. Lallart, "Recent progress in piezoelectric conversion and energy harvesting using nonlinear electronic interfaces and issues in small scale implementation," *Journal of Micromachines*, vol. 02, pp. 274-294, 2011.
- [66] S. B. Ahmed, G. Despesse, E. Defay and S. Boisseau, "Increased bandwidth of mechanical energy harvester," *Journal Sensors and Transducers*, vol. 13, pp. 62-72, 2011.
- [67] R. Caliò, U. B. Rongala, Camboni.D., M. Milazzo, C. Stefanini and G. d. Petris, "Piezoelectric energy harvesting solutions," *Sensors*, vol. 14, pp. 4755-4790, 2014.
- [68] F. P. Beer and E. R. Johnston, "Mechanics of Materials," *McGraw Hill Inc.*, 1992.
- [69] A. M. Flynn and S. R. Sanders, "Fundamental limits on energy transfer and circuit considerations for piezoelectric transformers," *IEEE Transactions on Power Electronics*, vol. 17, pp. 8-14, 2002.
- [70] R. C. Rosenberg and D. C. Karnopp, "Introduction to Physical System Dynamics," *McGraw Hill Inc.*, 1983.